*Handbook on the Physics and Chemistry of Rare Earths*
*Vol. 31*
*edited by K.A. Gschneidner, Jr., L. Eyring and M.B. Maple*


*Chapter 199*

# NEUTRON SCATTERING STUDIES OF LANTHANIDE MAGNETIC ORDERING

J.W. LYNN
*NIST Center for Neutron Research, National Institute of Standards and Technology, Gaithersburg, MD 20899, USA and Center for Superconductivity Research, Department of Physics, University of Maryland, College Park, MD 20742, USA*

S. SKANTHAKUMAR
*Chemistry Division, Argonne National Laboratory, Argonne, IL 60439, USA*

## Contents



## List of symbols

| | |
|---|---|
| 1-2-3 | $RBa_2Cu_3O_{6+x}$ |
| 2-4-8 | $R_2Ba_4Cu_8O_{16}$ |
| 2-4-7 | $R_2Ba_4Cu_7O_{15}$ |
| 2-1-4 | $R_{2-x}Ce_xCuO_4$ |
| 2D | two-dimensional |
| 3D | three-dimensional |
| $A$ | average size of domain in the $a$–$b$ layer |
| $a, b, c$ | lattice parameters |
| $C$ | instrumental constant for the calculation of neutron intensity |
| $F_M$ | magnetic structure factor |
| $f(\tau)$ | magnetic form factor |
| $h, k, l$ | Miller indices of Bragg peaks |
| $I(\tau)$ | neutron intensity at reciprocal lattice vector $\tau$ |
| $\boldsymbol{J}$ | total angular momentum |
| $J$ | exchange energy |
| $J_{ab}$ | exchange interaction energy in the $a$–$b$ plane |
| $J_c$ | exchange interaction energy along the $c$-direction |
| $k$ | Boltzmann constant |
| $\widehat{M}$ | unit vector along the spin direction |
| $\boldsymbol{q}_m$ | antiferromagnetic propagation vector |
| R | Lanthanide ion |
| RKKY | Ruderman–Kittel–Kasuya–Yosida |

| | | | |
|---|---|---|---|
| $S$ | total spin momentum | $\lambda$ | London penetration length |
| $S_i$ | spin operator at site $i$ | $\mu_B$ | Bohr magneton |
| $T$ | temperature | $\langle\mu_z\rangle$ | thermal average of the ordered magnetic moment |
| $T_c$ | superconducting transition temperature | | |
| $T_N$ | antiferromagnetic ordering (Néel) temperature | $\xi$ | superconducting coherence length |
| | | $\boldsymbol{\tau}$ | reciprocal lattice or scattering vector |
| $t$ | reduced temperature $(1 - T/T_N)$ | $\hat{\tau}$ | unit vector along the reciprocal lattice vector $\boldsymbol{\tau}$ |
| $\left(\frac{\gamma e^2}{2mc^2}\right)^2$ | neutron–electron coupling constant, $-0.27\times10^{-12}$ cm | | |

## 1. Introduction

The effects of magnetic impurities and the possibility of magnetic ordering in superconductors have had a rich and interesting history (see the reviews by Maple 1976 and Fischer and Maple 1983). Magnetic impurities substituted into a superconductor were found to quickly suppress superconductivity due to the strong spin scattering that disrupts the Cooper pairs. Typically ~1% substitution was enough to completely extinguish the superconducting state, and such a low concentration of magnetic moments precludes the possibility of cooperative magnetic states forming and competing with the superconducting order parameter. The first exception to this behavior was realized for the $(Ce_{1-x}R_x)Ru_2$ system, where over 30% of non-magnetic $Ce^{4+}$ could be replaced by the magnetic heavy lanthanides before superconductivity was suppressed. Strong ferromagnetic correlations were found to develop in the superconducting state, but no long-range order was present.

The first examples of true long-range magnetic order coexisting with superconductivity were provided by the ternary Chevrel-phase superconductors ($RMo_6S_8$) and related ($RRh_4B_4$) compounds (Fischer and Maple 1983). In these materials there is a separate, fully occupied lanthanide sublattice. The fact that these materials were superconducting at all implied that the magnetic ions and the superconducting electrons belonged to different, "isolated" sublattices, and thereby the conventional Abrikosov–Gorkov (1961) spin-depairing mechanism was suppressed. The magnetic ordering temperatures are all low, ~1 K, and thus it was argued that electromagnetic (dipolar) interactions should dominate the energetics of the magnetic system. For materials where these interactions favor antiferromagnetism the magnetization averages to zero on the length scale of a unit cell ($a$), which results in a weak influence on the superconducting state ($a \ll \xi, \lambda$). This is the most prevalent case found in nature, and apart from a few anomalies in properties such as the upper critical field, the antiferromagnetic order and superconductivity were found to readily accommodate one another. In the rare and more interesting situation where the magnetic interactions are ferromagnetic, there is strong coupling to the superconducting state that originates from the internally generated magnetic field. The competition with the superconducting order parameter gives rise to long wavelength oscillatory magnetic states and/or reentrant superconductivity; the neutron work has been

reviewed by Thomlinson et al. (1983), with some subsequent work (Lynn et al. 1984). The studies of these materials contributed greatly to our understanding of these two competing phenomena, but the possible role of exchange interactions in these systems, and the related question of how the dipolar interaction alone could be responsible for the antiferromagnetism in some materials while others (with the same crystal structure) are ferromagnets, remained unexplained.

The cuprate superconductors offer new and interesting perspectives into our understanding of "magnetic superconductors" for a number of reasons. In the materials typified by $RBa_2Cu_3O_{6+x}$ (1-2-3) and $R_2Ba_4Cu_8O_{16}$ (2-4-8), for example, the R ions appear to be electronically isolated from the Cu–O layers where the Cooper pairs form, similar to the ternary superconductors, and the low lanthanide ordering temperatures (~1 K) suggested that the cuprate superconductors were again prototypical "magnetic superconductors". They were also interesting because the layered crystal structure, with $c \approx 3a$, rendered them naturally two-dimensional (2D) in nature, and indeed some of the best 2D magnets known belong to this class of materials (see the review by Lynn 1992). However, there are also examples where the magnetic ordering temperature is much too high to be explained by dipolar interactions, and it has become clear that R–R exchange interactions actually must play a dominant role in the magnetism, as is also clearly the case for the new $RNi_2B_2C$ class of superconductors (Lynn et al. 1997, Stassis and Goldman 1997). In contrast to the ternary superconductors, in the cuprates there is no clear separation of the lanthanide sublattice from the superconducting electrons. Moreover, one of the most interesting aspects of the cuprates concerns the magnetism associated with the Cu ions, which is the same sublattice where the superconducting pairing occurs. The undoped cuprates are antiferromagnetic insulators where the $S = \frac{1}{2}$ Cu spins order at high temperatures, typically near or above room temperature. The in-plane Cu exchange interactions are much stronger than along the $c$-axis, and thus again the magnetism is two-dimensional in nature. With doping, the materials lose the Cu long-range magnetic order and become high-$T_c$ superconductors. However, the Cu moments and energetics are still present, and the essential role these quantum spin fluctuations play in the superconducting state is reviewed in ch. 198.

In the present chapter we review the neutron scattering investigations of the magnetic structures of the lanthanides in the cuprates. We start by discussing the tetragonal, single Cu–O layer electron-doped materials typified by $(Nd–Ce)_2CuO_4$. These are the simplest and best understood from a number of standpoints, but the lanthanide ions are clearly exchange coupled in these materials, and there is also an important coupling between the Cu and R moments. This is particularly evident when the Cu spins exhibit long-range order, and we will therefore briefly describe the nature of the Cu order as well, and its interaction with the lanthanide moments. We then discuss the 1-2-3- and 2-4-8-type layered materials, which often exhibit prototypical 2D behavior. Next we will turn to the behavior of the Pr ion in the cuprates, which is fundamentally different. In this case the 4f electrons hybridize with the conduction electrons, which results in Pr having the highest lanthanide ordering temperatures in this class of materials. This hybridization also typically extinguishes the superconductivity. Finally, we will summarize our overall

understanding of the lanthanide ordering in these materials, and briefly discuss future directions.

## 2. General trends

Before discussing the details of these materials, there are some general trends that should be noted. For the Cu spins, the central feature that controls many aspects of all the oxide materials is the strong copper–oxygen bonding, which results in a layered Cu–O crystal structure. In the undoped "parent" materials this strong bonding leads to an electrically insulating antiferromagnetic ground state. The exchange interactions within the layers are much stronger than between the layers, and typically an order-of-magnitude more energetic than the lattice dynamics. The associated spin dynamics and magnetic ordering of the Cu ions are thus driven by this two-dimensional nature. With electronic doping, long-range antiferromagnetic order for the Cu is suppressed as metallic behavior and then superconductivity appears, but strong antiferromagnetic spin correlations still persist in this regime. It is this large magnetic energy scale that is associated with the high superconducting transition temperature and exotic pairing, and these aspects are reviewed by Mason in ch. 198.

For the lanthanide magnetism, the overall behavior is quite different. In the single-layer $R_2CuO_4$ type materials the lanthanide exchange interactions are three-dimensional in nature, and typically the Cu and R systems exhibit relatively strong coupling. For the multi-layered materials, on the other hand, the distance along the stacking axis becomes quite large, and this physical separation renders the ordering two-dimensional in nature, but for very different reasons than for the Cu system. The R–Cu interactions also tend to be weaker and the lanthanide sublattice appears to be relatively isolated from the rest of the system, making them prototypical 2D magnets with low ordering temperatures.

In all of these systems, for both the Cu magnetic order as well as the lanthanide magnetic order, the spin structures are relatively simple commensurate antiferromagnetic configurations. In particular, no materials have been discovered yet that exhibit a net ferromagnetic component, with its associated macroscopic magnetization. By commensurate we mean that the antiferromagnetic unit cell is a simple integer multiple of the chemical unit cell. Within the Cu–O planes, for example, the nearest-neighbor spins have always been found to be antiparallel, and the spins always point along a common direction (i.e., they are collinear) within the $a$–$b$ plane. However, there can be the complication that some of the structures are noncollinear, by which we mean that the direction of the spins between the layers is not necessarily along the same crystallographic direction. The added complication of having both Cu and R moments can then make the magnetism of these cuprates quite rich and interesting.

## 3. Single-layer systems

We start our discussion with the magnetic ordering in the electron-type $R_2CuO_4$ (2-1-4) materials. The basic crystal structure is tetragonal *I4/mmm* (T′ phase) in which the Cu

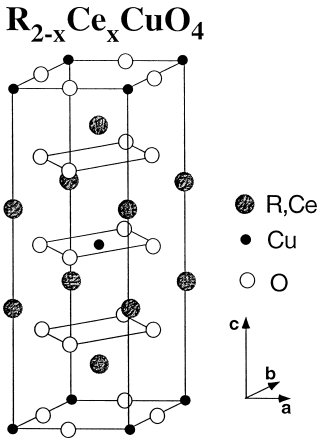


Fig. 1. T′ tetragonal crystal structure of the single Cu–O layer $R_2CuO_4$ system.

spins occupy a body-centered tetragonal (*bct*) lattice ($a \approx 3.91$ Å, $c \approx 11.9$ Å) as shown in fig. 1. The Cu–O bonding within the *a*–*b* plane results in strong exchange interactions within these layers, while the rare-earth ions form layers between these Cu–O planes. The Cu spins in the undoped ("parent") material are antiferromagnetically ordered and the material is insulating, while ~7.5% Ce or Th substituted onto the R site (R = Pr, Nd, Sm, Eu) gives the optimal doping for superconductivity, with $T_c \approx 25$ K. The phase diagrams as a function of doping for all of these cuprate materials are reviewed elsewhere in this Handbook (Maple 2000, Elschner and Loidl 2000). For the Cu spins the *c*-axis coupling is thus much weaker than the coupling in the *a*–*b* plane, giving rise to both two-dimensional magnetic properties and highly anisotropic superconducting behavior. Note, however, that the exchange interactions for both the Cu and R moments, as well as the superconducting order parameter, must be mediated through magnetically active layers.

When a material undergoes a transition from a paramagnet to a magnetically ordered state, new Bragg peaks develop that are associated with the long-range magnetic order. The positions of these new magnetic reciprocal lattice points $\boldsymbol{\tau}$ identify the magnetic configuration of the spins, while the size and spin direction of the moments can be determined from the intensities. For a simple collinear magnetic structure the neutron intensity is given by (Bacon 1975)

$$I(\boldsymbol{\tau}) = C \left( \frac{\gamma e^2}{2mc^2} \right)^2 \langle \mu_z \rangle^2 \, (f(\boldsymbol{\tau}))^2 \, |F_M|^2 \left\langle 1 - \left( \widehat{\tau} \cdot \widehat{M} \right)^2 \right\rangle, \tag{1}$$

where $C$ is an instrumental constant, the quantity in large parentheses is the neutron–electron coupling constant ($-0.27 \times 10^{-12}$ cm), $\langle \mu_z \rangle$ is the thermal average of the ordered magnetic moment, $f(\boldsymbol{\tau})$ is the magnetic form factor (the Fourier transform of the atomic magnetization density), $F_M$ is the magnetic structure factor, and $\widehat{\tau}$ and $\widehat{M}$ are unit vectors in the direction of the reciprocal lattice vector $\boldsymbol{\tau}$ and the spin direction, respectively. The orientation factor $\langle 1 - (\widehat{\tau} \cdot \widehat{M})^2 \rangle$ must be averaged over all possible

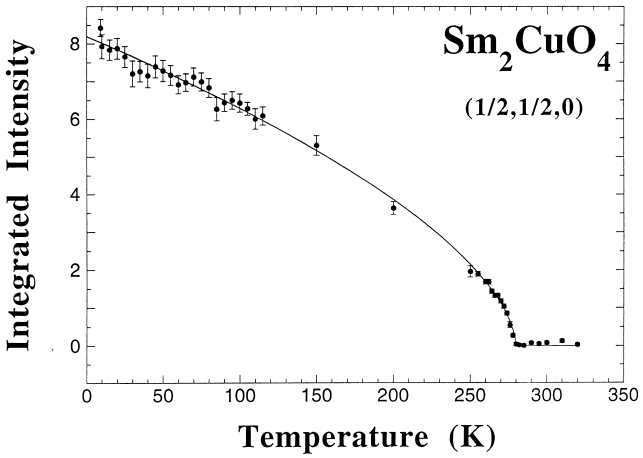


Fig. 2. Temperature dependence of the $(\frac{1}{2},\frac{1}{2},0)$ Cu magnetic Bragg peak in $Sm_2CuO_4$. The solid curve is a least-squares fit to a simple power law, $I = I_0(1 - T/T_N)^{2\beta}$, with $\beta = 0.30(1)$ and $T_N = 280(1)$ K (Skanthakumar et al. 1991).

domains. A similar, although more complicated, expression is obtained if the magnetic structure is noncollinear, but the general behavior in terms of magnetic moment, form factor, and determination of the spin directions is qualitatively the same.

Figure 2 shows the intensity of the $(\frac{1}{2},\frac{1}{2},0)$ magnetic Bragg peak associated with the Cu ordering in $Sm_2CuO_4$ (Skanthakumar et al. 1991). We see from eq. (1) that the intensity is proportional to the square of the ordered moment, which in this case is the sublattice magnetization. The smooth variation with temperature indicates that the ordered moment develops continuously below the Néel temperature of 280 K. However, we note that the intensity does not exhibit the usual saturation at low $T$ typical of a conventional three-dimensional order parameter. The solid curve is a fit to a power law $t^{2\beta}$, where $t$ is the reduced temperature and $\beta = 0.30 \pm 0.01$. This is the expected behavior near the ordering temperature, but it is unusual for a power law to fit the data over such a wide temperature range. This has been observed in other $S = \frac{1}{2}$ Cu–O systems, and is thought to originate from the two-dimensional quantum fluctuations present in these highly anisotropic antiferromagnets.

The magnetic Bragg peaks observed in the magnetically ordered state can be indexed as $(\frac{1}{2}h, \frac{1}{2}k, l)$ based on the chemical unit cell, where $h$ and $k$ are odd integers and $l$ is any integer. Since the first two Miller indices are half integers, the Cu magnetic unit cell is double the chemical unit cell along the $a$ and $b$ directions while it is the same along $c$. This Cu magnetic unit cell is the same as that found for the other 2-1-4 systems. The interactions between spins within an $a$–$b$ plane are antiferromagnetic as already discussed, so that nearest-neighbor spins within a layer are antiparallel, as is the case in all the cuprates. The nearest-neighbor exchange interaction $JS_i \cdot S_j$ between layers, on the other hand, is seen to cancel due to the body-centered tetragonal (*bct*) symmetry, further rendering the net Cu spin interactions 2D in nature. Hence the three-dimensional

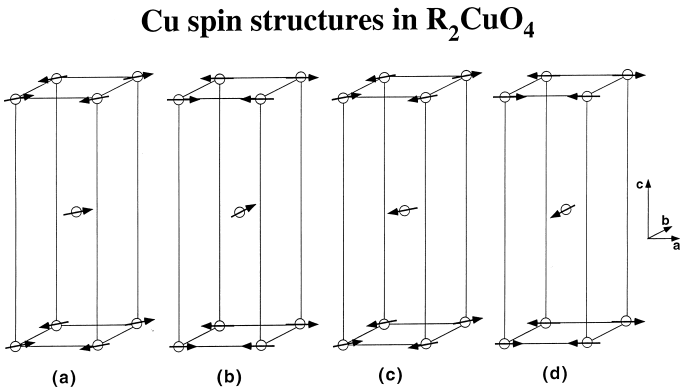


Fig. 3. The four possible Cu spin structures in tetragonal $R_2CuO_4$: (a) collinear with $\boldsymbol{q}_M \perp \widehat{M}$; (b) noncollinear-$Sm_2CuO_4$ type (c) collinear with $\boldsymbol{q}_M \parallel \widehat{M}$; (d) noncollinear-$Nd_2CuO_4$ type.

magnetic structure that is actually realized must be stabilized by higher-order interactions (Yildirim et al. 1996), as we will discuss shortly.

The detailed spin structure, which entails assigning a spin direction to each site, turns out to contain an ambiguity; there are two possible descriptions (figs. 3a,b) that may occur for the present case where the crystal structure has tetragonal symmetry, and it is not possible to distinguish between them with neutron diffraction data on a multidomain sample. One possibility is a collinear spin structure as shown in fig. 3a, which is the same structure as observed in orthorhombic $La_2CuO_4$ (Vaknin et al. 1987). The antiferromagnetic propagation vector $\boldsymbol{q}_{\mathrm{M}}$ that describes this structure is along the $[1\bar{1}0]$ direction, while the spin direction $\widehat{M}$ is orthogonal, along [110]. The structure then consists of ferromagnetic sheets in the (110) plane, with the spins in adjacent sheets antiparallel ($\boldsymbol{q}_{\mathrm{M}} \perp \widehat{M}$) and the magnetic symmetry is orthorhombic. A second, completely different possibility is the noncollinear spin assignments shown in fig. 3b. In this structure the spins within each Cu–O plane are again collinear and antiferromagnetically coupled as before, but the spins between adjacent planes are rotated by 90º and hence are noncollinear. The spin direction in this structure is either along the [100] axis or along the [010] axis, and the basic magnetic symmetry in this case is tetragonal rather than orthorhombic.

These two basic magnetic structures, collinear and noncollinear, are in fact closely related: the noncollinear structure can be obtained from the collinear structure by the *coherent* addition of two separate domains of the collinear structure. From a scattering point of view, the intensities of the magnetic Bragg peaks from a domain of the collinear structure would be quite different from those for the noncollinear structure. However, generally a material exhibiting the collinear structure would form equal populations of domains, and the intensities from the multiple-domain sample are identical to the intensities for the noncollinear structure. Thus in a zero-field experiment the two types of structures cannot be distinguished, and one must apply a symmetry-breaking magnetic field to identify the correct structure. If we apply the field along the [110] direction for

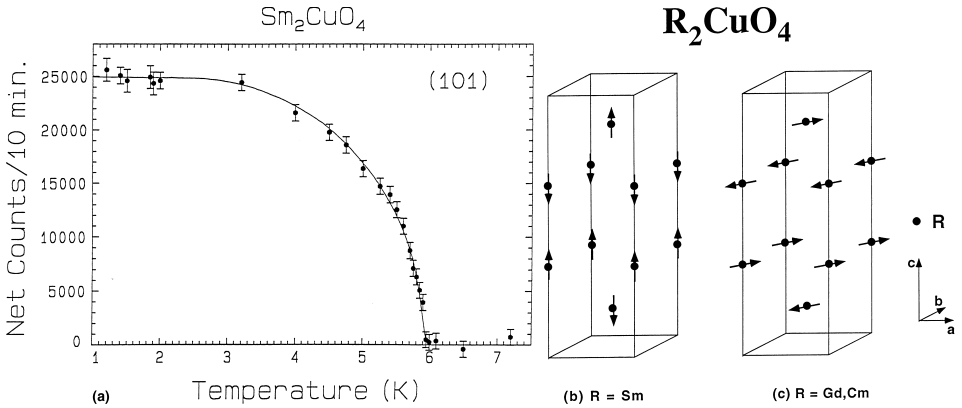


Fig. 4. (a) Temperature dependence of (1,0,1) Sm magnetic Bragg peak intensity (Sumarlin et al. 1992). (b) Sm magnetic structure. (c) Magnetic structure for Gd and Cm.

example, one can see from fig. 3 that the behavior of the spin system will be quite different depending on whether the structure is collinear, where spins are parallel or antiparallel to the field direction, or noncollinear, where the spins initially are at 45º to the field direction. The results for $Nd_2CuO_4$ (Skanthakumar et al. 1993a,b) demonstrate that the correct structure is the noncollinear one (Skanthakumar et al. 1989, Petitgrand et al. 1990), and the noncollinear structure appears also to be correct for $Sm_2CuO_4$ (Skanthakumar et al. 1993a), $Pr_2CuO_4$ (Sumarlin et al. 1995), and $Eu_2CuO_4$ (Chattopadhyay et al. 1994b).

For the lanthanide ordering, the simplest example is provided by $Sm_2CuO_4$, which also turns out to be an interesting example of the interaction between the lanthanide magnetism and superconductivity. All observed Sm magnetic peaks were found to coincide with nuclear peaks, and they can be indexed as (*h,k,l*) based on the chemical unit cell, where all *h, k* and *l* are integers and $h + k + l$ = even integer. The intensity of the [101] magnetic Bragg peak is shown in fig. 4a, where we find a Néel temperature of 5.95 K (Sumarlin et al. 1992). The magnetic transition is clearly very sharp, and indicates that the lanthanide and Cu magnetic structures do not interact significantly with each other. The fact that the Miller indices are integers signifies that the magnetic unit cell is identical to the chemical unit cell. The magnetic structure for the Sm moments is shown in fig. 4b, where we see that the moments form ferromagnetic sheets in the *a–b* plane, that are coupled antiferromagnetically along the *c*-axis, with the spin direction also along *c*. The Sm magnetic structure, which is in the I4/m′mm magnetic space group, then has a completely different symmetry than the Cu structure, and the spin directions are orthogonal as well, so that the two magnetic phases in this material are independent of each other to a very good approximation.

The ordered magnetic moment of the Sm ion is only $0.37(3)\mu_B$, which is quite small compared to the heavy lanthanides. With the high ordering temperature of ~6 K, it is quite clear that the energetics must be dominated by exchange interactions, with the dipolar interactions playing only a very minor role. In the doped superconducting

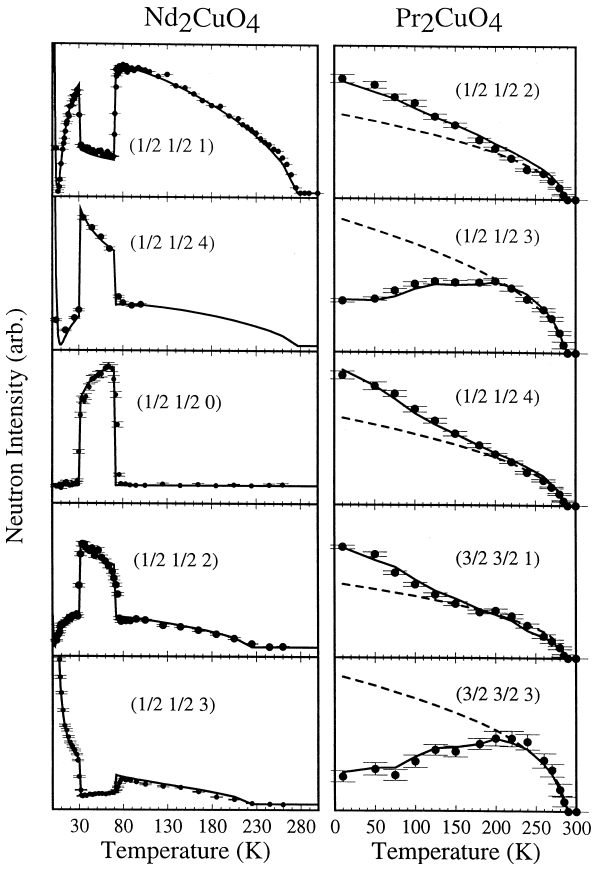


Fig. 5. (left) Temperature dependence of five $Nd_2CuO_4$ magnetic Bragg peaks (Skanthakumar et al. 1989, 1999). (right) Temperature dependence of five $Pr_2CuO_4$ magnetic Bragg peaks. The solid curves are fits to the theory (Sachidanandam et al. 1997); the dashed curves on the right show the contribution of the Cu spins to the intensities.

system, the dilution of the Sm sublattice smoothly decreases the Néel temperature to ~4.9 K, with little other effect on the magnetism. In the superconducting state ($T_c = 23$ K), but above the Sm antiferromagnetic ordering temperature, the Cu–O layers contain a mirror ($m$) symmetry, which the superconducting wave function must accommodate. When the Sm ions order magnetically, on the other hand, then the Cu–O layers contain an antimirror symmetry ($m'$), and the superconducting wave function must then accommodate this change in symmetry. Viewed along the $c$-axis, the system consists of alternating superconducting and ferromagnetic layers, which should require a change of sign of the superconducting order parameter in adjacent Cu–O layers. This "π-phase" model is predicted to substantially affect the superconducting state below the magnetic ordering temperature (Andreev et al. 1990), and this is an active area of interest both in this natural layered system and in artificially layered films.

The nature of the lanthanide moments and magnetic ordering can also have important consequences for the Cu magnetic structure, and vice versa, as we will now discuss. The column on the left of fig. 5 shows the temperature dependence of five magnetic

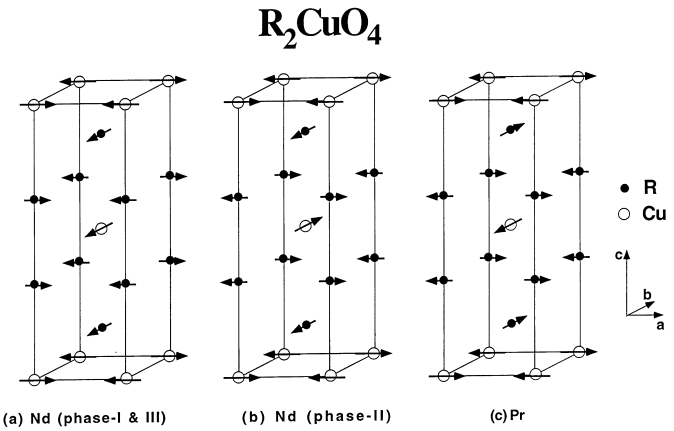


Fig. 6. Noncollinear spin structures for (a) Nd in phase I and III, (b) Nd in phase II, and (c) Pr.

Bragg peaks for $Nd_2CuO_4$. Five magnetic transitions have been identified (Skanthakumar et al. 1989, Endoh et al. 1989, Lynn et al. 1990, Matsuda et al. 1990). The initial ordering of the Cu spins occurs at a Néel temperature of 276 K for this sample, where all the $(\frac{1}{2},\frac{1}{2},l)$-type reflections increase in intensity with decreasing temperature in phase I ($75\,\mathrm{K} \leqslant T \leqslant 276\,\mathrm{K}$), and the noncollinear Cu spin structure is that shown in fig. 3d. We remark that the Cu ordering temperature is quite sensitive to small changes in the oxygen content, with $T_N$ varying from 245 K to 276 K (Skanthakumar 1993). At 75 K the intensities of the odd-integral (odd-$l$) peaks suddenly drop, while the even-integral peaks increase abruptly in intensity. This indicates that a spin-reorientation transition for the Cu spins has occurred, and the new noncollinear Cu spin structure is shown in fig. 3b. At 30 K another abrupt spin reorientation takes place, where the spins rotate back to the original spin sense as indicated by the negligible intensity for $T < 30\,\mathrm{K}$ of the $(\frac{1}{2},\frac{1}{2},0)$ peak, which has nonzero intensity only in Phase II ($30\,\mathrm{K} \leqslant T \leqslant 75\,\mathrm{K}$). Note that this is the same peak that has the strongest intensity for $Sm_2CuO_4$, and it turns out that these transitions are the result of a spin reorientation from one noncollinear structure to the other, and then back again, as shown in fig. 6. Similar types of spin-reorientation transitions have been observed in some other related compounds (e.g. $La_2CoO_4$), but those transitions are accompanied by structural phase transitions (Yamada et al. 1989). In $Nd_2CuO_4$, there is no evidence for structural phase transitions accompanying the magnetic order, and hence the origin of these spin-reorientation transitions must be different. Finally, the Nd ions order antiferromagnetically in the vicinity of 1.5 K, also in a noncollinear spin arrangement, and the magnetic symmetry of the Nd spins is identical to that of Cu spins. In addition to all these transitions, there is a fifth transition of a continuous nature at 0.15 K, which is due to an induced ordering of the nuclear spins through the hyperfine interactions. Such a nuclear spin ordering was originally introduced to explain the low-temperature data of both $Nd_2CuO_4$ and $Sm_2CuO_4$, and has been recently investigated thoroughly in $Nd_2CuO_4$ (Chattopadhyay and Siemensmeyer 1995).

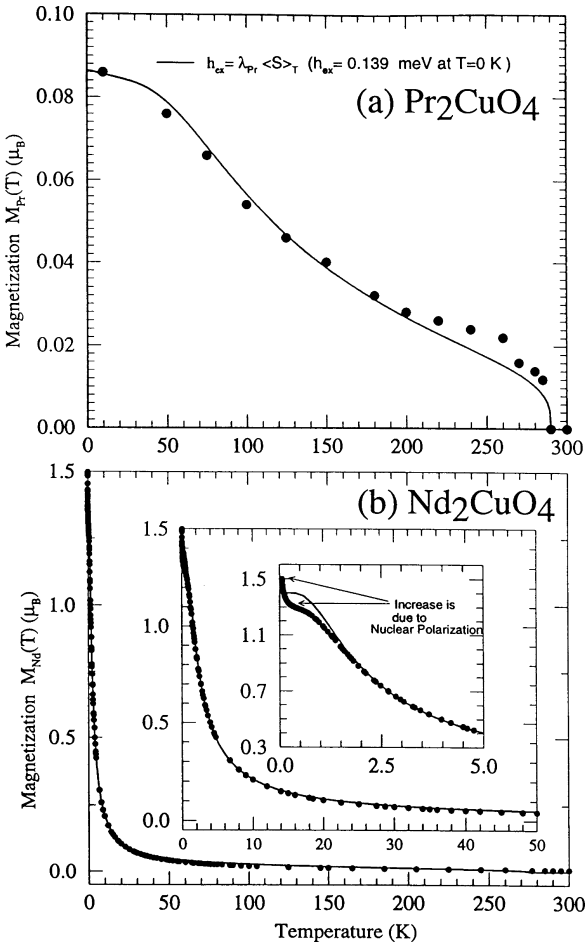


Fig. 7. Calculated polarization of the (a) Pr and (b) Nd moments in $R_2CuO_4$, via the interaction with the Cu ordered moments, as a function of temperature (Sachidanandam et al. 1997).

Below 30 K (phase III) the intensities evolve in a rather complicated way, and this turns out to be caused by the development of substantial (staggered) moments on the Nd sites as indicated in fig. 7b. Note in particular that the $(\frac{1}{2},\frac{1}{2},3)$ peak varies substantially in intensity at lower temperatures (fig. 5), and this is the strongest peak associated with the Nd ordering at low temperature (Lynn et al. 1990, Matsuda et al. 1990). The antiferromagnetically ordered Cu sublattice induces the Nd spins to order in a staggered arrangement. There are four Cu nearest-neighbor spins, one next-nearest-neighbor and four third-neighbors, for each Nd ion. The nearest-neighbor Cu–Nd interactions cancel exactly due to the tetragonal crystal symmetry. However, next-nearest-neighbor and third-neighbor interactions do not cancel, but instead produce a field that polarizes the Nd sublattice antiferromagnetically. This polarization field turns out to have the same symmetry as when the Nd ions order spontaneously, and thus the Nd ions are quite

susceptible even at elevated temperatures, and a net sublattice magnetization of the Nd ions is observed in all the ordered phases (fig. 7b). An induced Nd moment has also been observed in resonant X-ray scattering measurements (Hill et al. 1995). Magnetic structures for the Nd spins along with the Cu spins are shown in figs. 6a,b for all phases. Note that the induced moments at elevated temperatures (over 100 K), and the spontaneous order at low $T$, are noncollinear structures. Note also that the intensities of the $(\frac{1}{2},\frac{1}{2},1)$ and $(\frac{1}{2},\frac{1}{2},2)$ peaks increase with decreasing temperature in phase II, while the intensities of the $(\frac{1}{2},\frac{1}{2},0)$ and $(\frac{1}{2},\frac{1}{2},3)$ peaks decrease. This behavior is reversed in phase III, and these observations indicate that the Nd and Cu spins along the $c$-direction are coupled antiparallel in phase II, while they are parallel in phases I and III (figs. 6a,b). The temperature dependence of the other magnetic peaks as well as detailed refinements of the intensities (Skanthakumar 1993, Petitgrand et al. 1992) confirm this type of Nd–Cu coupling. The refined magnetic moment for Nd is 1.44, 0.04, and $0.014\mu_B$ at 0.4, 50 and 80 K, respectively. This shows in a direct way that the Nd and Cu spin systems are coupled, and because of the high temperatures involved this again must be exchange coupling rather than dipolar coupling. This has important implications for the superconductivity since the Nd moments and Nd ordering occur in the superconducting system; the conventional wisdom would say that the Abrikosov–Gorkov spin-depairing mechanism would surely destroy any chance for superconductivity in the material. Thus even if we were to discard the fact that there are Cu spin fluctuations in the superconducting phase of these materials, we still have to deal with the fact that the lanthanide moments are there, and are directly coupled through the superconducting planes.

The properties of both the Cu and lanthanide magnetic structures, ordered moments, and ordering temperatures are summarized in table 1, along with some related systems. For $Pr_2CuO_4$ the Cu spin structure (Cox et al. 1989, Allenspach et al. 1989, Matsuda et al. 1990, Sumarlin et al. 1995) is the same as that (fig. 3d) observed in $Nd_2CuO_4$ at high temperature. The temperature dependence of five typical magnetic peaks is shown in the right-hand column of fig. 5, where we see that the nonmonotonic behavior again indicates that R–Cu coupling is also present in $Pr_2CuO_4$. The spin structure is shown in fig. 6c, and the (small) induced Pr moment (obtained from theory discussed below) is shown in fig. 7a. We see that the Pr and Cu spins are coupled antiferromagnetically along the $c$-direction, in contrast to $Nd_2CuO_4$. Measurements under high pressure in $Pr_2CuO_4$ suggest spin-reorientation transitions (Katano et al. 1993) similar to $Nd_2CuO_4$, but the Nd system is the only one to exhibit these under ambient pressure. For $Eu_2CuO_4$, the $Eu^{3+}$ ion has a non-magnetic ground state, and therefore only Cu magnetic ordering is observed in this system (Chattopadhyay et al. 1994b, Gukasov et al. 1992). In $Gd_2CuO_4$ (Chattopadhyay et al. 1991b, 1992) and $Cm_2CuO_4$ (Soderholm et al. 1999), the lanthanide and Cu spin structures are different. Gd and Cm order ferromagnetically in the $a$–$b$ plane and are coupled antiferromagnetically along $c$ like $Sm_2CuO_4$, with relatively high ordering temperatures. However, the spin direction is in the $a$–$b$ plane, and the easy direction within this plane cannot be obtained by (zero-field) neutron data. Note that superconductivity does not occur in these two compounds for any Ce doping. Finally, we note that there

Table 1
Magnetic properties of $R_2CuO_4$ [a]. The Cu ordering temperature, $T_N$(Cu), and ordered moment, $\mu_{Cu}$, change with oxygen concentration. Here we give the highest observed $T_N$ and the corresponding $\mu_{Cu}$

| Material | $T_N$(Cu) (K) | $\mu_{Cu}$ ($\mu_B$) | Magnetic structure, Cu | $T_N$(R) (K) | $\mu_R$ ($\mu_B$) | Magnetic structure, R | Ref. |
|---|---|---|---|---|---|---|---|
| $La_2CuO_4$ [b] | 325 | 0.5 | fig. 3a | | | | 1 |
| $Pr_2CuO_4$ | 284 | 0.40(2) | fig. 3d | Induced | 0.080(5) | fig. 6c | 2–5 |
| $Nd_2CuO_4$ | 276 | 0.46(5) | fig. 3d [c] | ~1.5 | 1.44(5) | fig. 6a | 4,6–14 |
| $Sm_2CuO_4$ | 280 | 0.38(4) | fig. 3b | 5.95(5) | 0.37(3) | fig. 4b | 8,15–17 |
| $Eu_2CuO_4$ | 265 | 0.4(1) | fig. 3b | | $J \equiv 0$ | | 18,19 |
| $Gd_2CuO_4$ | 285 | | fig. 3c or d | 6.4 | 7 | fig. 4c | 20,21 |
| $Cm_2CuO_4$ | | | [d] | 25 | 5.0(5) | fig. 4c | 22 |
| $Sr_2CuO_2Cl_2$ | 251 | 0.34(4) | fig. 3a or b | | | | 23,24 |
| $Ca_2CuO_2Cl_2$ | 247 | 0.25(10) | [e] | | | | 25 |

[a] La, Eu, Sr and Ca ions do not a carry magnetic moment. The ground state of Pr is a nonmagnetic singlet and only a small induced moment is observed for Pr due to exchange mixing.
[b] Only $La_2CuO_4$ has an orthorhombic (Cmca) crystal structure; all others are tetragonal (I4/mmm). However, recently orthorhombic structural distortions have been reported in $Eu_2CuO_4$ and $Gd_2CuO_4$ (Vigoureux et al. 1997a,b).
[c] Spin reorientation occurs at 75 K and 30 K. Between these two temperatures the correct structure is represented by fig. 3b.
[d] Cu ordering in $Cm_2CuO_4$ has not been studied yet, but the Cu spin structure is not expected to be different from other $R_2CuO_4$ compounds.
[e] Cu spin structure is different from all other related materials. In this system, the magnetic unit cell is doubled along the *c*-direction.

*References*

[1] Vaknin et al. (1987); review: Lynn (1990)
[2] Cox et al. (1989)
[3] Allenspach et al. (1989)
[4] Matsuda et al. (1990)
[5] Sumarlin et al. (1995)
[6] Skanthakumar et al. (1989)
[7] Skanthakumar et al. (1993a)
[8] Skanthakumar et al. (1993b)
[9] Lynn et al. (1990)
[10] Endoh et al. (1989)
[11] Chattopadhyay et al. (1991a)
[12] Akimitsu et al. (1989)
[13] Rosseinsky et al. (1989)
[14] Petitgrand et al. (1990)
[15] Skanthakumar et al. (1991)
[16] Skanthakumar (1993)
[17] Sumarlin et al. (1992)
[18] Gukasov et al. (1992)
[19] Chattopadhyay et al. (1994b)
[20] Chattopadhyay et al. (1991b)
[21] Chattopadhyay et al. (1992)
[22] Soderholm et al. (1999)
[23] Vaknin et al. (1990)
[24] Yildirim et al. (1998)
[25] Vaknin et al. (1997)

is an indication for an induced Gd moment due to the polarization by the Cu sublattice in $Gd_2CuO_4$ (Chattopadhyay et al. 1994a), and in principle the Cu sublattice polarizes rare-earth spins in all these compounds. Superconductivity does not occur in any of the other $R_2CuO_4$ (R = Tb–Lu) systems, and no neutron diffraction experiments have been reported yet.

The effects of Ce doping on the magnetic ordering of R and Cu in $R_{2-x}Ce_xCuO_4$ have been studied for the Nd and Pr systems (Lynn et al. 1990, Skanthakumar et al. 1992, 1999, Skanthakumar 1993, Thurston et al. 1990, Rosseinsky et al. 1991, Zobkalo et al. 1991). Taking $Nd_{2-x}Ce_xCuO_4$ as an example, for small Ce concentrations ($x < 0.14$) the same non-collinear antiferromagnetic order (fig. 6) for both the Cu and Nd spins is observed. Both the average ordered Cu moment and $T_N$ decrease with increasing Ce concentration $x$, and no long-range order is observed at optimal doping of $x = 0.15$ (7.5% substitution of Ce for Nd). The Cu spin-reorientation transitions also broaden rapidly with increasing $x$, while the fraction of Cu spins that participate in the spin reorientation also appears to decrease with increasing $x$.

On the other hand, the Nd ordering transition, which is smeared due to the strong Cu–Nd coupling in $Nd_2CuO_4$, becomes sharper with increasing $x$. The temperature dependence of the $(\frac{1}{2},\frac{1}{2},3)$ magnetic peak for crystals with various Ce concentrations is shown in fig. 8a. Since the ordered Cu moment decreases with increasing $x$, the strength of the Nd–Cu coupling and the associated induced moment also decrease with increasing $x$, allowing the transition to become sharper. To see this effect directly, the temperature dependence of the ratio between the ordered moments of Nd and Cu for various Ce concentrations is shown in fig. 8b. In the temperature regime where the dominant contribution to the Nd ordered moment is via the Nd–Cu interaction, these temperature-dependent moment ratios fall on a universal curve since the induced Nd moment is proportional to the ordered Cu moment. The proportionality constant depends on the magnetic susceptibility of the Nd ions, and we see that the Nd contribution to the magnetic susceptibility changes only marginally with cerium doping. At lower temperatures ($< 1.5$ K), the ordered Nd moment develops a contribution from the Nd–Nd interaction, and the ratios for different Ce concentrations depart from the universal curve. Nuclear spin ordering of Nd also contributes to the increase in intensity below ~0.4 K.

In the superconducting sample ($x = 0.15$), there is no indication for long-range Cu magnetic ordering. However, a transition to long-range antiferromagnetic order of Nd occurs at 1.2 K, with an ordered moment of $0.85\mu_B$, and this transition is relatively sharp as there is no ordered Cu moment to induce Nd ordering at higher temperatures. There is no indication for long-range ordering of either Cu or Nd in crystals with higher cerium concentrations ($x > 0.17$). However, at low temperatures, broad magnetic peaks with weak intensities due to short-range Nd order are observed. The intensities of these peaks are found to increase with decreasing temperature, analogous to an order parameter, while the widths are approximately temperature independent. This indicates that for higher cerium concentrations the domains are small (~150 Å).

Oxygen plays a crucial role in both the magnetic and transport properties of the high temperature superconductors. In the electron-doped $Nd_{2-x}Ce_xCuO_4$ system the superconducting properties were found to be very sensitive to both cerium and oxygen concentrations. In fact, even in optimally doped $Nd_{1.85}Ce_{0.15}CuO_4$, superconductivity can be achieved only by removing a small amount of oxygen from as-grown samples (Radaelli et al. 1994) and not by doping more Ce. The overall effects of oxygen reduction on the Cu magnetic ordering are similar to that of increasing the cerium concentration in

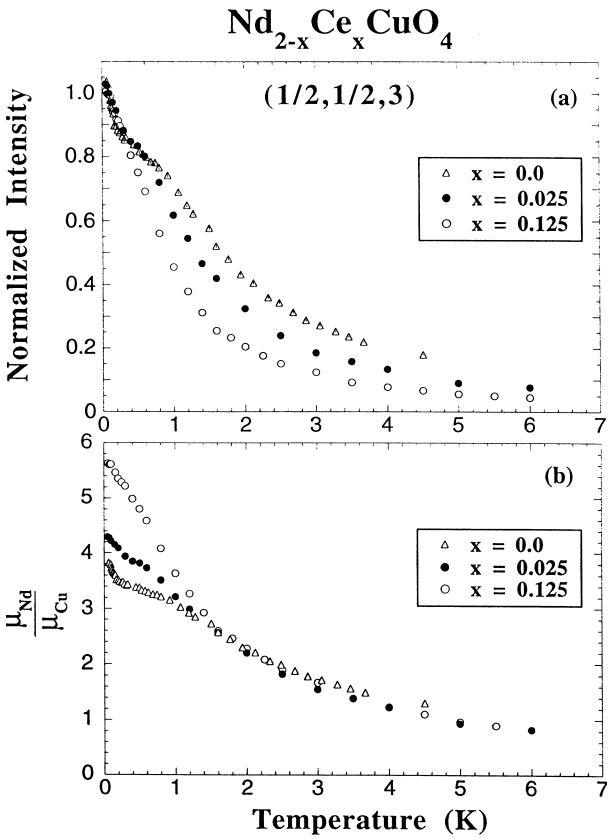


Fig. 8. (a) Temperature dependence of the $(\frac{1}{2},\frac{1}{2},3)$ magnetic Bragg peak for $Nd_{2-x}Ce_xCuO_4$ crystals with various Ce concentrations. (b) Temperature dependence of the ratio between the ordered moments of Nd and Cu. At higher temperatures, the ordered (induced) Nd moment is proportional to the Cu moment, and thus the curves for various crystals overlap. At lower temperatures (below 1.5 K), the Nd ions spontaneously order (Skanthakumar 1993, Skanthakumar et al. 1999).

$Nd_{2-x}Ce_xCuO_4$ (Skanthakumar 1993, Matsuda et al. 1992). In $Nd_{1.85}Ce_{0.15}CuO_4$, the observed magnetic intensities due to Nd ordering in as-grown samples were found to be larger than those of the deoxygenated (superconducting) samples. In addition, magnetic ordering of Cu and, therefore, the Nd–Cu coupling, are observed in as-grown samples, while they disappear when the excess oxygen is removed.

As mentioned earlier, the linear exchange interaction between Cu layers cancels due to the *bct* symmetry, and the actual spin structure is then a result of a delicate balance of superexchange, spin–orbit, and Coulomb exchange interactions (Yildirim et al. 1994, 1996). In the absence of the R ions, quantum fluctuations would be expected to yield the collinear magnetic structure (Yildirim 1999) and this may indeed be the case for the $Sr_2CuO_2Cl_2$ material (Yildirim et al. 1998). However, this leaves unexplained the

observation of the noncollinear structures in the $R_2CuO_4$, and quantum fluctuations certainly cannot explain the series of spin rotations that occur in $Nd_2CuO_4$. It is thus clear that the lanthanide exchange interactions and crystal-field anisotropies must play an essential role in determining the three-dimensional magnetic structures realized in these systems, and the correlation between lanthanide magnetism and superconductivity.

Considerable progress in properly taking into account the lanthanide exchange interactions and crystal field anisotropies has been achieved recently (Yildirim et al. 1994, Sachidanandam et al. 1997). The theory includes various novel anisotropic magnetic interactions in the cuprates that have a microscopic origin, along with R–R, R–Cu, and Cu–Cu exchange interactions. The calculations show that due to the exchange field acting on the lanthanide ion coupled with the crystalline electric field interactions, there is a strong single-ion anisotropy that orients both the Cu and R = Pr, Nd spins along the [100]-type directions, into the observed noncollinear spin arrangement. The model also successfully predicts the consecutive spin flop transitions observed in $Nd_2CuO_4$, and the calculations (solid curves) shown in fig. 5 are in excellent agreement with the data. The Cu spins order first, and then as the temperature decreases the Nd spins develop a significant polarization. As this polarization develops it disrupts the balance of energies along the *c*-axis, and this causes an abrupt (first-order) spin reorientation from one noncollinear structure to the other. As the Nd moment increases the energetics shift again and the spins rotate back to their original directions. The polarization of the Nd sublattice, as determined by fitting the model to the intensities of a series of magnetic Bragg peaks, is shown in fig. 7b. We see that there is a substantial induced moment on the Nd below ~100 K, while the Nd exchange orders the moments at ~1.5 K (in the absence of the Cu). This behavior contrasts with the situation for $Pr_2CuO_4$, where the Pr crystal-field ground state is a (non-magnetic) singlet (Sumarlin et al. 1995, Staub and Soderholm 2000). There is then a small moment that is present due to exchange mixing (Matsuda et al. 1990, Sumarlin et al. 1995), and the polarization of this moment as determined from the model is presented in fig. 7a; the excellent fits to the data are shown as solid curves in the right column of fig. 5. The model predicts that there is significant polarization all the way up to $T_N$(Cu), but this polarization is too small to cause spin reorientations in $Pr_2CuO_4$, in agreement with experiment. Finally, we note that this same type of calculation also predicts that the easy axis lies along [001] for Sm in $Sm_2CuO_4$, with no significant coupling of the lanthanide and Cu spin structures, again in agreement with observation. We conclude then that there is a good overall understanding of the microscopic magnetic interactions, and the consequent magnetic phases and associated spin dynamics, in the single-layer materials.

## 4. Multilayered systems

We have seen in the previous section that the single-layer materials exhibit substantial R–Cu exchange coupling, and they also have modest (for cuprates) superconducting transition temperatures. For the materials that contain multiple Cu–O layers the $T_c$ values

are typically much higher because of the stronger coupling between the Cu–O layers. For the canonical $RBa_2Cu_3O_{6+x}$ (1-2-3) system, there are three copper–oxygen layers of ions in each chemical unit cell, which are stacked along the *c*-axis. Two of these layers have oxygen ions between the Cu ions in both the *a* and *b* crystallographic directions (the Cu-plane layers), and the oxygens cannot be removed. The third Cu layer only has O ions along one axis. This is the so-called "chain layer", and the oxygen concentration can be readily varied in this layer from full occupancy ($x = 1$) to full depletion ($x = 0$). Both the magnetic and superconducting properties are very sensitive functions of the oxygen concentration *x*; in the fully oxygenated case ($x = 1$) the system is a $90^+$ K superconductor for all the trivalent lanthanide elements R except Pr, while in the magnetic regime ($x \leqslant 0.4$) the Cu plane-spins order antiferromagnetically and the system is a Mott insulator.

The lanthanide ions are centered between the two Cu plane layers in the 1-2-3 system, but they turn out to be remarkably isolated electronically from the Cu–O layers. Indeed all the physical measurements on the $RBa_2Cu_3O_{6+x}$ (1-2-3), the $R_2Ba_4Cu_8O_{16}$ (2-4-8), and the $R_2Ba_4Cu_7O_{15}$ (2-4-7) systems show that the 4f electrons are effectively isolated from the Cu–O superconducting layers, as well as from each other. The single exception is for Pr, and we will discuss this unique case separately. The crystal-field splittings are also very important (except for Gd), and for the orthorhombic symmetry appropriate for these materials typically the lanthanide ground state is doubly degenerate for half-integral *J* (like Dy or Er) or singly degenerate (like Ho) for integral *J* (and hence non-magnetic). The crystal-field properties have been reviewed by Staub and Soderholm (2000). As far as the nature of the magnetic ordering is concerned for half-integral *J*, the higher crystal-field levels are at energies much larger than the ordering energy $kT_N$, and consequently do not play an important role in the ordered state. However, the first excited state for integral *J* is very close to the ground state (except for Tm), and therefore it is possible for the rare-earth ions to order magnetically in these materials as well. In Tm, the singlet ground state is well separated from higher states (~12 meV), and consequently lanthanide magnetic order is not observed in the Tm compounds. For the systems with a magnetic ground state the direct (exchange) overlap of the 4f wave functions is of course out of the question, and the indirect and superexchange interactions turn out to be relatively small. Thus the ordering temperatures are low (typically ~1 K), and dipolar interactions are important in these materials. Hence the lanthanide magnetism is similar in many regards to "conventional" magnetic-superconductor systems.

The sublattices for the lanthanide ions are shown in fig. 9 for the 1-2-3 (9a), 2-4-8 (9b), and 2-4-7 (9c) structures. Neglecting the small orthorhombic distortion in the *a*–*b* plane, the 1-2-3 lattice is simple tetragonal. The 2-4-8 system then consists of two 1-2-3 unit cells stacked on top of one another, but shifted by *b*/2. The 2-4-7 system, on the other hand, consists of two 1-2-3 cells stacked directly on top of one another, and then another two layers stacked on top, but shifted by *b*/2. Hence the 2-4-7 structure consists of 1-2-3 bilayers. The basic ingredient that lowers the effective dimensionality *d* of this class of magnetic materials to $d = 2$ is that for all three structures the nearest-neighbor R distance along the *c*-axis is three times the nearest-neighbor distance in the *a* or *b* directions; typically $a \approx b \approx 3.9$ Å, and $c \approx 12$ Å. For a dipolar interaction

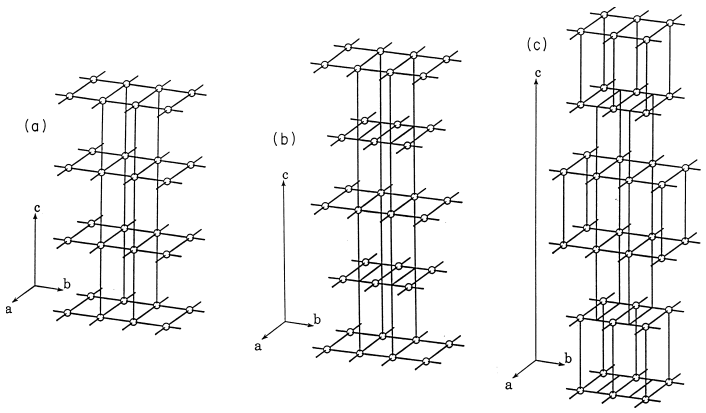


Fig. 9. Crystal structures for the rare-earth ions in the (a) 1-2-3, (b) 2-4-8, and (c) 2-4-7 systems. The two-dimensional behavior of the magnetism is due to the large inter-ion spacing along the $c$-axis compared to the $a$–$b$ plane ($c \approx 3a$). In addition, in the 2-4-8 and 2-4-7 structures the net interactions along the $c$-axis cancel for some magnetic configurations.

($E \propto 1/r^3$) the strength of the coupling along $c$ should be reduced by $\sim(a/c)^3 \approx 1/27$, while either direct or superexchange interactions would be expected to be reduced by even a larger factor. A significant indirect (RKKY) exchange might still be operative over this long distance, but the conduction electron density at the lanthanide site turns out to be small, and in fact the ordering temperatures in both the insulating and superconducting compounds (which in the 1-2-3 materials can be realized by simply varying the oxygen content) are comparable. The final conclusion is that the interaction along $c$ is indeed considerably more than an order of magnitude smaller than the interactions operating within the $a$–$b$ plane, and this generates the 2D-like magnetic behavior. This contrasts with the interactions in the 2-1-4 materials, where the nearest-neighbor R distances are all comparable, and there is no 2D-like behavior for the R magnetism.

### 4.1. *Cu spin ordering*

The high-temperature antiferromagnetic transition in the 1-2-3 system involves the ordering of the Cu spins in the Cu-plane layers. At $x = 0$ the Néel temperature $T_N$ can exceed 500 K, and then $T_N$ monotonically decreases to zero at $x \approx 0.4$. The spins within the $a$–$b$ plane are antiferromagnetically aligned, as is always the case, with the spin direction also in the $a$–$b$ plane. The Cu ions in adjacent layers are located immediately above and below each other along the $c$-axis, and the exchange interaction along the $c$-axis is also antiferromagnetic. In particular, the Cu lattice is not body-centered as in the single-layer materials, and hence there is no cancellation of the exchange interactions between layers. Nevertheless, the overall behavior is still quite 2D in nature because of the strong in-plane Cu-O bonding. It is also possible to dope the chain layers in the 1-2-3 material electronically, either from adjacent sites or directly on the Cu chains, and this can cause a moment to develop on the Cu chain sites, which can also order. This is not a problem for

the heavy lanthanides, but is an important difficulty encountered in the Pr system, and to a lesser extent in Nd 1-2-3. This coupling breaks the symmetry that the lanthanide site enjoys when only the Cu-plane layers are magnetic, and can consequently influence the lanthanide ordering and R–Cu coupling. We will return briefly to this problem when we review the Pr ordering.

For the 2-4-8 materials we note that it is not possible to vary the oxygen content significantly, while for the 2-4-7 systems it can be varied from 14 to 15. However, there is no long-range Cu order to consider in these superconducting systems.

### 4.2. *Lanthanide ordering in $RBa_2Cu_3O_7$*

The R–R interactions in these superconductors are all quite weak, and the antiferromagnetic ordering temperatures are typically ~1 K as already noted. The most thoroughly investigated system is probably $ErBa_2Cu_3O_7$, and this material turns out to be an ideal representation of a $S = \frac{1}{2}$ 2D Ising antiferromagnet. Early investigations were carried out on polycrystalline samples (Lynn et al. 1987), and were followed by detailed studies on single-crystal samples (Lynn et al. 1989, Paul et al. 1989, Chattopadhyay et al. 1988a, 1989). In the top portion of fig. 10 we present a diagram of reciprocal space, showing the positions of the nuclear (crystal structure) and magnetic (spin structure) Bragg peaks which occur at positions like $(\frac{1}{2}h,k,\frac{1}{2}l)$. If the system were purely 2D in character then we would expect to see rods of magnetic scattering as shown; above the ordering temperature this scattering originates from critical fluctuations, while below $T_N$ it originates from low-energy spin waves. The lower portion of fig. 10 shows three scans through the rod, just above the ordering temperature. This strong rod of scattering develops for temperatures $\leqslant 1$ K, and at the temperature shown the width is solely instrumental in origin. Also shown in the figure is a scan along the rod, which demonstrates that the scattering intensity is essentially uniform. Hence there are no significant correlations between the spins in adjacent $a$–$b$ layers, even though we are just above $T_N = 0.62$ K as indicated by the measured sublattice magnetization shown in fig. 11. The energetics are clearly 2D in nature, and we thus regard the phase transition at $T_N$ as 2D in character.

The magnetic structure for Er 1-2-3 is shown in fig. 12a, and consists of chains of spins coupled ferromagnetically along the $b$-axis, and antiferromagnetic along $a$ and $c$. The in-plane magnetic structure is found to be identical in the Er 2-4-8 and Er 2-4-7 systems. In the Dy (Goldman et al. 1987, Fischer et al. 1988, Clinton et al. 1991), Nd (Yang et al. 1989, Fischer et al. 1989), and Gd (Paul et al. 1988) 1-2-3 superconductors, on the other hand, nearest-neighbor spins are found to be antiparallel in all three directions, and they exhibit the magnetic structure shown in fig. 12c, with ordering temperatures of 0.9, 0.5, and 2.2 K, respectively. Tb does not form the 1-2-3 structure, but superconducting $TbSr_2Cu_{2.7}Mo_{0.3}O_7$ exhibits the same magnetic structure, with $T_N = 5.4$ K (Li et al. 1997). Tm 1-2-3, on the other hand, possesses a singlet crystal-field ground state, which must be non-magnetic. This illustrates an important point, that the crystal field plays an essential role in these systems (see ch. 194 of Vol. 30 of this Handbook, by Staub and Soderholm). The above four ions (Er, Dy, Gd, and Nd) are half-integral $J$ lanthanide ions, and therefore

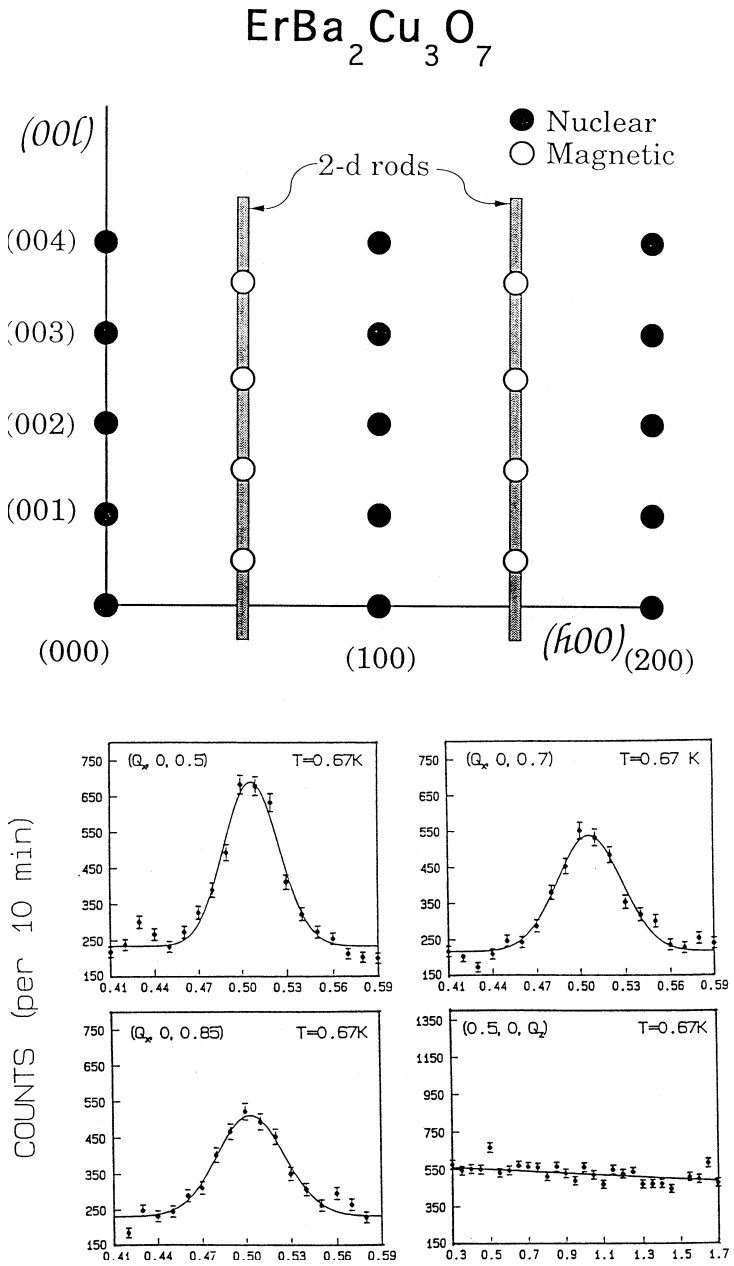


Fig. 10. (top) Reciprocal space for $ErBa_2Cu_3O_7$, showing the three-dimensional nuclear and magnetic Bragg peaks, and the two-dimensional rods of scattering. (bottom) Scans through the rod, and along the rod, just above the ordering temperature of 0.618 K, showing that there are strong spin correlations within the *a–b* planes, but no significant correlations between planes (Lynn et al. 1989).

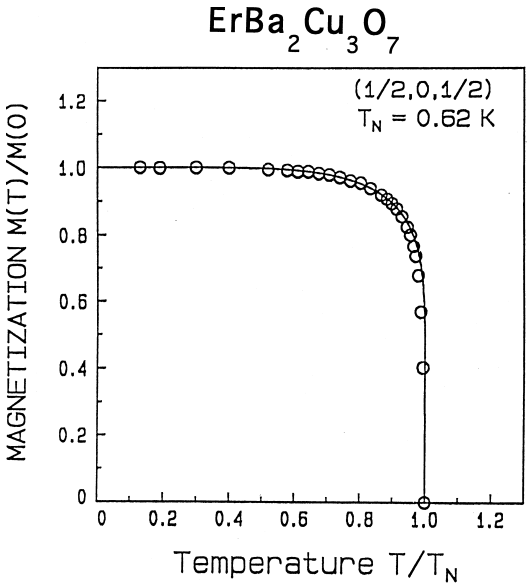


Fig. 11. Temperature dependence of the sublattice magnetization for $ErBa_2Cu_3O_7$. The solid curve is the fit to the data of Onsager's exact solution for the $S=\frac{1}{2}$, 2D Ising model (Lynn et al. 1989).

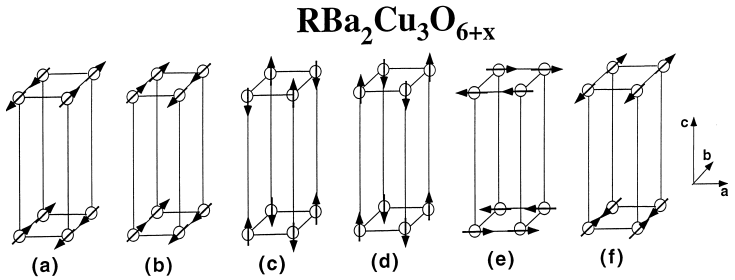


Fig. 12. Three-dimensional magnetic structures for the $RBa_2Cu_3O_{6+x}$ systems. (a) $ErBa_2Cu_3O_7$ (Lynn et al. 1987, 1989, Paul et al. 1989, Chattopadhyay et al. 1988a, Maletta et al. 1990, Clinton et al. 1995). (b) The Er spins in portions of some samples of $ErBa_2Cu_3O_{6+x}$ are coupled ferromagnetically along the $c$-axis (Chattopadhyay et al. 1988a, 1989, Paul et al. 1989, Clinton et al. 1995). (c) $DyBa_2Cu_3O_7$ (Goldman et al. 1987, Fischer et al. 1988, Clinton et al. 1991, 1995), $NdBa_2Cu_3O_{6+x}$ (Yang et al. 1989, Clinton et al. 1995), $PrBa_2Cu_3O_{6+x}$ (Li et al. 1989, Guillaume et al. 1993), $GdBa_2Cu_3O_{6.14}$ (Mook et al. 1988, Paul et al. 1988) and $TbSr_2Cu_{2.69}Mo_{0.3}O_7$ (Li et al. 1997). (d) $DyBa_2Cu_3O_6$ (Guillaume et al. 1993, Clinton et al. 1995), $GdBa_2Cu_3O_{6+x}$ (Chattopadhyay et al. 1988b, Guillaume et al. 1993). (e) Correlations in $HoBa_2Cu_3O_7$ (Roessli et al. 1993a). (f) $YbBa_2Cu_3O_7$ (Roessli et al. 1992).

in a (low-symmetry) crystal-field environment we expect the ground state to be (at least) doubly degenerate (so that $S=\frac{1}{2}$ is appropriate). Consequently the lanthanide ions will always carry a moment at low temperatures, and order magnetically. This is also the case for Yb 1-2-3, which orders antiferromagnetically at 0.4 K (Roessli et al. 1992). The situation for the case where $J$ is whole-integral, on the other hand, results in a crystal-field ground state that is a (non-magnetic) singlet. Hence Tm 1-2-3 does not order

(Chattopadhyay et al. 1990). Ho also does not have a conventional magnetic transition, but the large nuclear moment and hyperfine field combine to drive a phase transition at 140 mK (Roessli et al. 1993a).

It is important to note that the dimensionality of the phase transition is also evident in other measurements such as specific heat and susceptibility, which measurements in fact often precede the neutron experiments and play an essential role in detecting the phase transition and revealing the nature of the magnetism. Specific heat as well as inelastic neutron scattering have also shown that the crystal-field ground state for the Er ion (as well as Dy and Nd) is a doublet, so that an $S = \frac{1}{2}$ (two-state) description is appropriate. Hence this system should be described by an $S = \frac{1}{2}$ 2D Ising antiferromagnet. Below the Néel temperature Bragg scattering is observed, and the temperature dependence of the sublattice magnetization (order parameter) is shown in fig. 11. The solid curve in the figure is the exact Onsager (1944) result for the $S = \frac{1}{2}$ 2D Ising model, and it is seen that experiment is in excellent accord with this exact theory. Analogous behavior has been observed in $DyBa_2Cu_3O_7$ (Clinton et al. 1991, 1995).

One of the interesting features of "2D" magnetic systems is that generally they will order three-dimensionally even if the interaction in the third direction is very weak (see Lynn 1992 for a review). To understand the origin of this behavior, we designate $J_{ab}$ to be the basic interaction within the $a$–$b$ plane, which will consist of possible exchange plus dipolar energies, and $J_c$ as the energy (likely dominated by dipolar interactions) of interaction along the $c$-axis. The crystallography for the present systems dictates that $J_{ab} \gg J_c$, and hence the systems should display 2D-like behavior. By this we mean that for $kT \gg J_{ab}$ there will be no significant correlations in the system, and the magnetic (diffuse) scattering will be uniformly spread throughout the entire Brillouin zone. As $kT$ becomes comparable to $J_{ab}$, strong correlations develop within the planes, while there will be no significant correlations between layers as has been found in the $ErBa_2Cu_3O_7$ and $DyBa_2Cu_3O_7$ systems just discussed. This will give rise to rods of critical scattering. For $J_{ab} > kT > J_c$ we will continue to see a rod of scattering; above the ordering temperature this will be critical scattering, while below the ordering temperature this will consist of low-energy spin waves.

For systems which are strictly two-dimensional, of course, only an Ising model (which we believe to be appropriate for the present materials) will exhibit true long-range order at finite temperature. However, even for the cases of $xy$ or Heisenberg spins, 3D long-range order will be induced for $J_c \ll J_{ab}$. In the conventional two-dimensional systems such as $K_2NiF_4$ (Birgeneau et al. 1970) and $K_2CoF_4$ (Ikeda and Hirakawa 1974), and of course the Cu spins in the insulating cuprates, the 2D ordering and the 3D ordering in fact occur at (essentially) the same temperature. The reason for the induced 3D order can be understood by the following argument. Assume that a static moment has developed in the layers. There is then an energy $\pm J_c A$ between the layers, where $A$ is the average size of a domain in the layer. The minus sign is for layers that are properly matched (e.g. antiferromagnet configuration if $J_c < 0$), where every spin is correctly paired with the adjacent layer. The + sign, on the other hand, is for layers that are mismatched,

in which every spin is incorrectly aligned. Thus even if the interlayer coupling is very weak, there is an energy difference ~$2J_cA$ between the "correct" and the "wrong" spin configurations, and this energy difference can be quite large since $A$ is large. Hence as soon as 2D order is established, ordering is expected to be induced along the $c$-axis, producing 3D Bragg peaks. In the "conventional" 2D magnets studied to date, in fact, no difference has been discerned between $T_N$(2D) and $T_N$(3D). An interesting exception to this behavior will be discussed in the next section.

Another manifestation of the weak interactions along the $c$-axis is that the materials can get "confused" about what is the correct spin structure. The confusion may be caused by the influence of twin and grain boundaries, defects, intergrowths, variations in the oxygen content, etc., which can alter the delicate balance of the dipolar energies. The $ErBa_2Cu_3O_7$ structure, for example, corresponds to chains of moments that are aligned ferromagnetically along the $b$-axis, while adjacent chains are aligned antiparallel to form an overall antiferromagnetic configuration. In some samples, however, the spins along the $c$-axis are found to be parallel rather than antiparallel, forming ferromagnetic sheets of spins (Paul et al. 1989, Chattopadhyay et al. 1988a, 1989). The dipole energies for these two configurations are very similar, and the specific structure may depend on the metallurgical state of the sample. A similar dichotomy of structures has been observed for the Dy (Clinton et al. 1991, 1995, Goldman et al. 1987) and Gd (Mook et al. 1988, Chattopadhyay et al. 1988b) 1-2-3 compounds, and a multiplicity of magnetic structures may be a common feature of these systems. The magnetic structures for the 1-2-3 materials are summarized in fig. 12; additional details are reviewed elsewhere (Lynn 1990). Dipole–dipole interactions favor three different types of magnetic order in the $a$–$b$ plane based on the direction of the magnetic moment, which is generally determined by the crystal-field anisotropy. If the moment is along the $c$-axis (Nd, Gd, Dy), nearest-neighbor spins order antiferromagnetically along both $a$ and $b$ directions (figs. 12c,d). If moments are along the $b$-axis (Er), they are coupled antiferromagnetically along $a$ and ferromagnetically along $b$ (figs. 12a,b), and this coupling is reversed for moments along the $a$-axis (fig. 12e) (Ho; Roessli et al. 1993a). All the $a$–$b$-plane spin configurations are the same for 2-4-7, 2-4-8, and for 1-2-3 compounds with different oxygen concentrations; the only known exception to this is Yb (Roessli et al. 1992), where the magnetic moment is along $b$ like Er, but the coupling is ferromagnetic along $a$ and antiferromagnetic along $b$ (fig. 12f).

### 4.3. *$R_2Ba_4Cu_8O_{16}$ and $R_2Ba_4Cu_7O_{15}$ systems – ideal 2D magnetism*

The 2-4-8 and 2-4-7 systems are directly related to the 1-2-3 system, and the lanthanide sublattices are shown in fig. 9 (above). For the 2-4-8 system which we will discuss first, the basic difference with the 1-2-3 is that each layer along the $c$-axis is shifted by $b/2$, producing a face-centered type of lattice along the $b$-axis. The nearest-neighbor distance along the $c$-axis is still three times $a$ or $b$, and hence the intrinsic magnetic interactions are highly anisotropic just like the 1-2-3 case. The low-temperature magnetic diffraction pattern for a powder sample of $Dy_2Ba_4Cu_8O_{16}$ (often called simply $RBa_2Cu_4O_8$) is

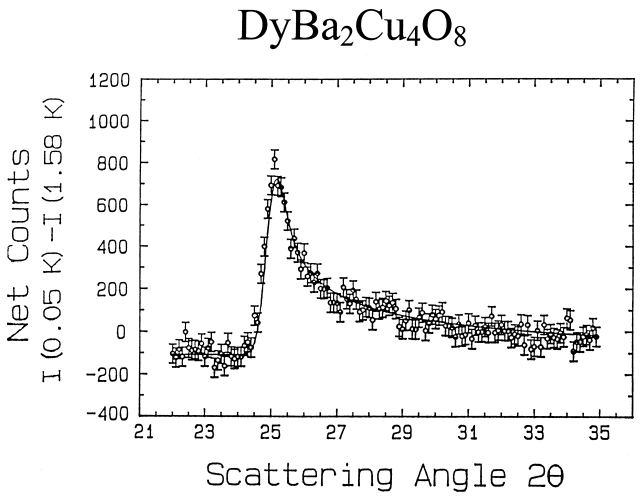


Fig. 13. Magnetic scattering for $DyBa_2Cu_4O_8$ at 0.05 K, well below the ordering temperature of 0.9 K. The data are obtained by subtracting the high temperature data from the data well below the ordering temperature, and the "negative" background is due to the absence of paramagnetic scattering in the ordered state. The magnetic scattering exhibits the classic shape for a two-dimensionally ordered material. No three-dimensional Bragg peaks are observed at any temperature (Zhang et al. 1990).

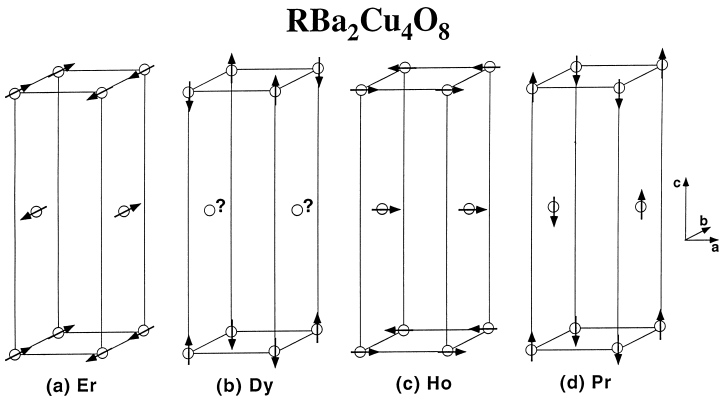


Fig. 14. Magnetic structures for the $RBa_2Cu_4O_8$ materials. (a) Er (Zhang et al. 1990). (b) Dy (Zhang et al. 1990, Roessli et al. 1993b). (c) Ho (Roessli et al. 1994). (d) Pr (Lin et al. 1998).

shown in fig. 13 (Zhang et al. 1990). Instead of 3D powder Bragg peaks, the scattering shows a 2D-like "sawtooth" profile even though we are well below the Néel temperature $T_N = 0.9$ K. The solid curve is in fact a fit to the 2D theory, assuming long-range order within the $a$–$b$ plane and no correlations along the $c$-direction. The scattering corresponds to the $(\frac{1}{2},\frac{1}{2})$ 2D peak, which means that nearest neighbors within the $a$–$b$ plane are antiparallel. The magnetic structure for Dy 2-4-8 (Zhang et al. 1990, Roessli et al. 1993b) is shown in fig. 14b, along with the other 2-4-8 systems investigated. In the first layer all

the spins are antiferromagnetically arranged. In the next layer up along the *c*-axis, all the spins are displaced by *b*/2. For the closest spins between layers, we will have two + spins and two − spins, and the net interaction is zero. Next-neighbor interactions also cancel, and in fact all the (point) interactions sum to zero by symmetry. Hence this is an example of a fully frustrated spin system for the interlayer coupling (indicated by the question mark in the figure), and the *a*–*b* layers are for practical purposes completely decoupled from one another. Similar behavior has been observed in the $Dy_2Ba_4Cu_7O_{15}$ system (Zhang et al. 1992). In this bilayer case the magnetic scattering appears as a modulated saw-tooth profile, with the modulation arising from the bilayer structure of the material. We expect a similar decoupling of adjacent layers or bilayers for any of the other lanthanide elements which have the same in-plane magnetic structure, which is in fact the most common occurrence. For $Er_2Ba_4Cu_8O_{16}$, on the other hand, the Er spins in the *a*–*b* plane form ferromagnetic chains (Zhang et al. 1990), as in the Er 1-2-3 case. This magnetic structure does not possess the frustration of the Dy material, and thus conventional three-dimensional Bragg peaks are observed below $T_N$. However, above $T_N$ 2D correlations are still found, indicating that the basic interactions are 2D-like as expected.

Three-dimensional magnetic Bragg peaks are also observed in $Er_2Ba_4Cu_7O_{14.92}$ (Böttger et al. 1997), with a finite but large correlation length (~130 Å) along the *c*-axis. Specific-heat data on this compound can be described by an anisotropic 2D Ising antiferromagnet, and therefore the basic interactions are 2D in character like Er 1-2-3 and Er 2-4-8. The only other compound in this series that has been studied by neutron diffraction is Ho 2-4-8 (Roessli et al. 1994). The data are similar to Dy 2-4-8, and thus Ho 2-4-8 is fully frustrated for the interlayer coupling; the data show long-range 2D magnetic peaks with a short correlation length (~18 Å) along the *c*-axis.

### 4.4. *Oxygen dependence of the lanthanide ordering in* $RBa_2Cu_3O_{6+x}$

Significant variations of the magnetic ordering are observed as a function of oxygen concentration for various lanthanides, such as Er (Clinton et al. 1995, Maletta et al. 1990), Dy, and Nd (Clinton et al. 1993, 1995), while in $GdBa_2Cu_3O_{6+x}$ the oxygen concentration does not appear to affect the nature of the three-dimensional long-range magnetic order or the ordering temperature (~2.2 K) (Chattopadhyay et al. 1988b, Paul et al. 1988, Mook et al. 1988). In $ErBa_2Cu_3O_{6+x}$, for example, $T_N$ is initially found to decrease with decreasing $x$, and for $x \gtrsim 0.5$ long-range 3D magnetic order occurs below $T_N$ and 2D short-range correlations above $T_N$. For $x \lesssim 0.5$ 3D long-range magnetic order is lost, and only 2D correlations are observed. In $ErBa_2Cu_3O_6$, neither 2D nor 3D long-range order develops, and only 2D short-range correlations are observed. The superconducting phase of $DyBa_2Cu_3O_{6+x}$ exhibits the same behavior as Er, that is, no 3D correlations are observed above $T_N$ (~0.9 K), while 3D long-range order is observed below $T_N$. In the insulating phase ($x < 0.4$), on the other hand, both 2D and 3D correlations develop at low temperatures, but 3D long-range order never occurs.

The concentration of oxygen appears to have the strongest effects in $NdBa_2Cu_3O_{6+x}$ (Yang et al. 1989, Clinton et al. 1993, 1995). For the fully oxygenated (and supercon-

ducting) materials 3D long-range order is observed, with $T_N = 0.53$ K. Modest reduction of the oxygen concentration to $x = 0.78$, however, completely destroys 3D order, and only short-range 2D correlations (~20 Å) are observed. At lower $x$ where the insulating phase occurs (and the Cu spins are ordered) 3D order again develops with a $T_N$ as high as 1.5 K. The transition is still sharp, as there is not much coupling to the Cu sublattice. The ordered moment for Nd is only about $1\mu_B$, so the high ordering temperature for Nd cannot be explained by dipole interactions alone.

All these observations indicate that there is some coupling between lanthanide moments and the Cu chain layer, since the magnetic ordering is strongly affected by the oxygen content. The detailed nature of these interactions, however, is not understood at this time.

### 4.5. $Pb_2Sr_2R_{1-x}Ca_xCu_3O_8$

Neutron studies (Wu et al. 1994, 1996, Hsieh et al. 1994b, Staub et al. 1995–1997) have been performed on the magnetic ordering in powder samples of $Pb_2Sr_2R_{1-x}Ca_xCu_3O_8$, which superconducts for $0.2 < x < 0.8$. In these materials all the lanthanides except Ce superconduct, with $T_c$ as high as 80 K. The suppression of superconductivity in $Pb_2Sr_2Ce_{1-x}Ca_xCu_3O_8$ is not thought to be connected to the magnetism, but to the tetravalent nature of the Ce ion in this compound (Skanthakumar and Soderholm 1996).

The lanthanide ions in this system have a site environment that is similar to that in the 1-2-3 systems, and the 2D magnetic behavior that has been observed for R = Tb and Pr is not unexpected. The separation along the $c$-axis is about 15.8 Å, which is even larger than the 1-2-3 system. In $Pb_2Sr_2Tb_{1-x}Ca_xCu_3O_8$, the Tb spins are found to order with relatively high transition temperatures of 5.3 and 4 K for $x = 0.0$ and 0.5, respectively. These high ordering temperatures again demonstrate that exchange interactions dominate in these materials. In addition, magnetic susceptibility and inelastic neutron scattering experiments suggest that significant 2D Tb–Tb correlations persist even at temperatures above the superconducting transition temperature, which is more than an order of magnitude above $T_N$. Further work on this class of materials is warranted.

## 5. The special case of Pr

A singular exception to the low ordering temperatures of the lanthanides is found for the class of cuprates that contain Pr: these generally are not even metallic let alone superconducting. This unique behavior has inspired extensive studies of the physical properties of the Pr cuprates in order to determine why only Pr suppresses the superconducting state while the other lanthanides exhibit very little effect. The magnetic ordering of the Pr is also anomalous in that the ordering temperatures are an order of magnitude higher (~15 K) than for the other rare-earth systems, indicating much stronger exchange and hybridization effects for the 4f Pr electrons.

Investigations of the magnetic order of Pr in $PrBa_2Cu_3O_{6+x}$ have been complicated by a number of factors. One is that this material is a semiconductor for all $x$, and thus

the Cu spins always order at a much higher temperature than the Pr spins. A second complication is that with appropriate doping, either directly on the chain site or on the Ba site, the chain spins can also develop a moment and exhibit long-range magnetic order, either together with the plane spins or as a separate magnetic transition. Moreover, the development of chain moments turns out to be especially sensitive to even small levels of dopants in the Pr 1-2-3 system, which has been a particular problem with many flux-grown crystals. A further complication is that the ordered moments for Pr and Cu are comparable in magnitude, and this can lead to ambiguities in the interpretation of data. Finally, Pr has a tendency to occupy the Ba site in Pr 1-2-3, and this changes both the magnetic and electronic behavior.

These complications have led to possible ambiguities in interpretations and lively debates, but a consensus has now emerged about the nature of the Pr ordering in these materials. Nevertheless, the consensus is certainly not yet unanimous, and the debate will no doubt continue with the recent report by Zou et al. (1998) of superconductivity in a small fraction of a variant, not yet identified, phase of Pr 1-2-3. This contrasts with the semiconducting behavior found in the overwhelming majority of Pr 1-2-3 samples, as already noted. However, it has been shown that the susceptibility in the sample that exhibits superconductivity is a factor of two smaller than was reported initially (Narozhnyi and Drechsler 1999, Zou et al. 1999), suggesting that the Pr content is reduced by half, and thus it seems likely that the floating-zone technique produces small regions that are either Y-rich and/or Ba-rich with Ba occupying the Pr site. In particular, it is known that relatively modest substitution for Ca on the Pr site provides a 90 K superconductor (Xiong et al. 1998), and similar behavior would be expected for Ba. Thus it seems likely that the superconductivity does not originate from Pr 1-2-3, but rather from an alloy.

We start our discussion of the Pr magnetic ordering by considering $PrBa_2Cu_3O_{6+x}$, which was the first Pr material to be investigated with neutrons (Li et al. 1989). The system is a semiconductor for the full range of $x$, with the Cu ions retaining their high magnetic ordering temperature. The f-electron hybridization has been observed directly by inelastic neutron scattering experiments, which have found that there are substantial linewidths to the crystal-field excitations of the Pr (Staub and Soderholm 2000). The exchange interactions are thereby enhanced, increasing the ordering temperature and rendering the lanthanide ordering 3D in nature.

In this initial study a simple antiferromagnetic ordering was found to develop below $T_N = 17$ K, with antiferromagnetic coupling between nearest-neighbor Pr moments in all three directions in the crystal. The magnetic structure is the same as found in the Dy and Gd 1-2-3 systems, shown in fig. 12c. The observed ordering temperature was in good agreement with specific heat and susceptibility results, which studies have elucidated the systematics of this ordering by following it as a function of oxygen concentration and as a function of Y (and other lanthanides) substitution on the Pr site (for a review see Radousky 1992). Bulk measurements show that as oxygen is removed $T_N$(Pr) monotonically decreases to 12 K for $PrBa_2Cu_3O_6$, and this has been confirmed by neutron diffraction measurements on the depleted system (Guillaume et al. 1993).

Studies on single crystals of the "pure" $PrBa_2Cu_3O_{6+x}$ have been carried out subsequently, but the results have been complicated because of contamination of the samples from the crucible, and/or Pr substitution on the Ba site. In particular, it is now known that crystals grown in alumina or MgO crucibles by the flux technique become doped by Al or Mg (Casalta et al. 1994, Uma et al. 1998b). These (inadvertent) dopings can cause the Cu chain spins to order (Lynn et al. 1988, Li et al. 1988, 1990, Rosov et al. 1992a). This ordering varies with oxygen content *x,* and is strongly coupled to the Pr sublattice because the symmetry of the two magnetic structures is the same. The chain doping can also reduce the Néel temperature for the Pr ordering, and can change the nature of the Pr structure along the *c*-direction (Longmore et al. 1996, Boothroyd et al. 1997, Boothroyd 1998, 2000) so that the usual *c*-axis antiferromagnetic coupling is not found in these samples. During the course of these investigations there was also a suggestion from NMR measurements (Nehrke and Pieper 1996) that the Pr was actually non-magnetic in pure Pr 1-2-3, but a reinvestigation with neutrons (Skanthakumar et al. 1997b) on pure powders indicated that the Pr was indeed ordering, and this has also been confirmed on pure crystals by neutrons (Uma et al. 1998a) and by resonant X-ray scattering (Hill et al. 1998). It therefore appears likely that the NMR may have been detecting some Pr on the Ba site in that sample, which may well be in a nonmagnetic singlet crystal-field state, while the line due to the Pr on the R site is too broad to observe.

The relatively recent development of non-reactive $BaZrO_3$ crucibles has now permitted the growth and investigation of undoped single crystals. In a fully oxygenated single crystal the Cu spins order at 281 K, while the Pr moments order at 16.8 K as shown in fig. 15 (Uma et al. 1998a). The initial ordering is revealed by the intensity of the $(\frac{1}{2},\frac{1}{2},0)$ versus $T$ shown in the center. This structure corresponds to antiferromagnetic alignment of spins in the *a–b* plane, while the spins along the *c*-direction are ferromagnetically aligned. The development of the ordered Pr moment is accompanied by a modest coupling to the Cu spins as indicated by the intensity of the $(\frac{1}{2},\frac{1}{2},2)$ Cu peak (top). At ~11 K (on cooling) a first-order "spin-flop" transition occurs to a Pr spin structure where the nearest-neighbor Pr moments along the *c*-axis flip to become antiparallel rather than parallel. This corresponds to the development of the $(\frac{1}{2},\frac{1}{2},\frac{1}{2})$-type peak as indicated in the bottom of the figure. The data clearly indicate that there is strong hysteresis in both types of Pr magnetic peaks, and the behavior is in good agreement with the specific heat and thermal expansion data taken on warming and cooling. The results on this pure single crystal are in general agreement with the data obtained on the polycrystalline sample, but the details with regard to the crossover from ferromagnetic to antiferromagnetic nearest-neighbor alignment along the *c*-axis are different. These differences are likely due to the delicate balance of interactions along the *c*-axis (Narozhnyi et al. 1999), and their subtle dependence on factors such as small concentrations of defects and impurities, oxygen content, strain, etc. There have also been indications of a small in-plane incommensurability of the magnetic peaks observed by X-ray resonant scattering (Hill et al. 1998).

Studies have also been carried out to observe the effects on both Cu and Pr order by chemical substitution on other sites in the Pr 1-2-3 system. Zn is found to substitute on

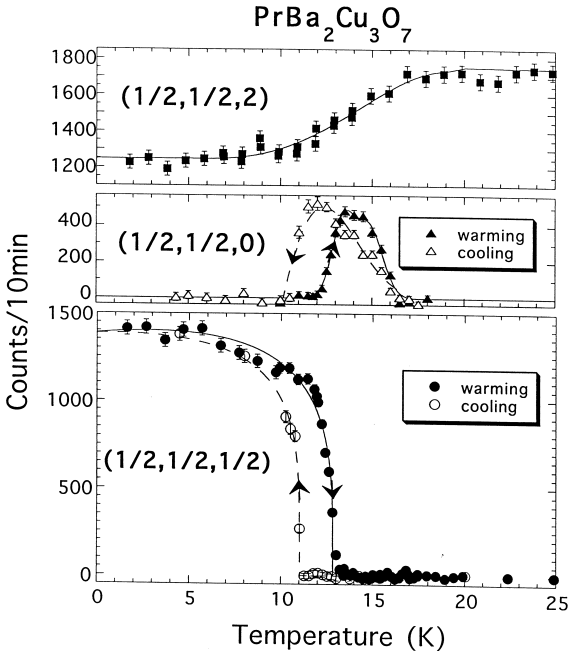


Fig. 15. Temperature dependence of the (top) $(\frac{1}{2},\frac{1}{2},2)$, (center) $(\frac{1}{2},\frac{1}{2},0)$, (bottom) $(\frac{1}{2},\frac{1}{2},\frac{1}{2})$ magnetic Bragg peaks in a pure single crystal of $PrBa_2Cu_3O_7$ (Uma et al. 1998a).

the Cu planes, and this has no effect on either the Pr ordering temperature or size of the ordered moment (Li et al. 1993), but it does change the coupling along the *c*-axis from antiferromagnetic to ferromagnetic. Ga, on the other hand, substitutes preferentially on the Cu chain sites. This again changes the magnetic structure along the *c*-axis from antiferromagnetic to ferromagnetic, but in addition $T_N$ is reduced (Li et al. 1994) while the ordered moment remains unchanged. Neither of these substitutions has a significant effect on the Cu powder Bragg peaks in the temperature regime where the Pr orders. Another type of substitution can occur for "pure" $PrBa_2Cu_3O_{6+x}$, where the Pr can substitute on the Ba site forming $Pr_{1+x}Ba_{2-x}Cu_3O_{6+y}$. This has the effect of reducing the ordering temperature for the Pr (Malik et al. 1992), as does La substitution for Ba (Wang et al. 2000).

There has been considerable additional work investigating the magnetic ordering of the Pr in the cuprate class of materials, and the properties for Pr systems investigated with neutrons in this class of materials have been reviewed recently elsewhere (Lynn 1997). $PrBa_2Cu_4O_8$ also orders antiferromagnetically at $T_N \approx 17$ K like the 1-2-3 material, with an analogous magnetic structure (Lin et al. 1998, Li et al. 1999). For $PrBa_2Cu_2NbO_8$ (Rosov et al. 1993) the Cu chain layer is replaced with a (fully oxygenated) $NbO_2$ layer, which of course carries no moment. This eliminates the complication of the chain magnetism, and we still find a high ordering temperature for the Pr and no influence on the Cu plane ordering when the Pr subsystem orders. A similar situation occurs for $TlBa_2PrCu_2O_7$ (Hsieh et al. 1994a) where the CuO chains are replaced by TlO.

There is no observable interaction between the Cu and Pr order, as would be expected since the magnetic structures have different symmetries. Similar behavior is observed for the more complicated $Pr_{1.5}Ce_{0.5}Sr_2Cu_2(Nb,Ta)O_{10}$ system (Goodwin et al. 1997). Again there can be no Cu chain magnetism, and there is a high observed $T_N$ for the Pr. The $Pb_2Sr_2PrCu_3O_8$ material (Hsieh et al. 1994b, Lin et al. 1997) is somewhat different in that it has no oxygen in the Cu chain layer, while the properties of the Pr are quite similar to the other systems. Finally, we note that the related $BaPrO_3$ material, which obviously has no complications of Cu ordering of any kind, exhibits a similar Pr ordering temperature and reduced moment (Rosov et al. 1992b) as for the cuprates. Thus in all the layered cuprates the Pr carries a moment and orders magnetically at much higher temperatures than the heavy lanthanides.

## 6. Lanthanide spin dynamics

Measurements of the spin dynamics of the lanthanide moments are considerably more difficult than determining the magnetic structures, but several investigations have been made which we briefly point out. If we introduce lanthanide exchange interactions, then this will give rise to magnetic excitons propagating in the lattice. This is revealed as dispersion of the crystal-field levels, and such dispersion has been observed for both $Pr_2CuO_4$ (Sumarlin et al. 1994, 1995) and $Nd_2CuO_4$ (Henggeler et al. 1996), and for the Ce-doped systems (Henggeler et al. 1997). The observed dispersion is as large as a few meV, which indicates that there are quite significant R–R exchange interactions in these materials. The spin dynamics of the exchange-split crystal-field ground state have also been investigated for $Nd_2CuO_4$ by Loewenhaupt et al. (1995), and more recently by Casalta et al. (1998) above the Nd magnetic ordering temperature. The latter authors find that there is a fluctuation component that persists up to room temperature, and is associated with the exchange field of the Cu spins acting on the Nd moments. This has decidedly 2D character and presumably originates from the 2D character of the Cu spin system. The other component originates from the usual paramagnetic spin fluctuations of the Nd moments above the ordering temperature. Below $T_N$ the Nd and Cu modes are predicted to be mixed in the parent compound, and the theoretical predictions for the spin dynamics in the ordered state (Thalmeier 1996, Sachidanandam et al. 1997) are in reasonable agreement with experiment (Henggeler et al. 1997). There is predicted to be an additional mode that has yet to be observed, and additional work in this area is desirable. In the doped system the observed spin waves are simplified because the Cu spins are not ordered, and the model calculations are able to reproduce the data.

The spin dynamics of the lanthanide systems have also been investigated both above and below the ordering temperature in superconducting $ErBa_2Cu_3O_7$ (Skanthakumar et al. 1997a). In this case the Cu moments interact weakly with the Er and are not ordered, and the lanthanide system can thus be treated independently of the Cu. The ground-state dispersion relation along the [110] direction is shown in fig. 16. There is a large (compared to $kT_N$) gap of about 0.20 meV in the excitation spectrum, as would be

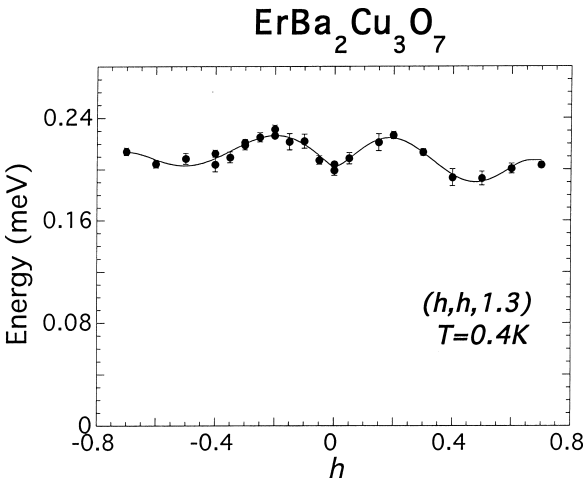


Fig. 16. Spin wave dispersion along [110] direction for $ErBa_2Cu_3O_7$. The solid curve is a guide to the eye (Skanthakumar et al. 1997a).

expected for an Ising system. However, for a pure Ising system $S^z$ commutes with the Hamiltonian and thus the spin waves would be dispersionless, while there is clearly some observed dispersion in the $a$–$b$ plane. Measurements along the $c$-axis indicate that these excitations have no measurable dispersion in that direction, and this behavior is expected because the magnetic interactions are weak along the $c$-direction. The Ising-type gap is still dominant, though, and the data of fig. 16 show that this material is still a good approximation to an Ising magnet.

Finally, we note that the spin dynamics for the Pr 1-2-3 system have been investigated in some detail, and not surprisingly, it is quite different than the other systems. A broad distribution of quasielastic scattering (and broad crystal field levels) was observed in powders (Skanthakumar et al. 1990). These energy widths could be due to exchange interactions, where the width is caused by the powder average of a dispersive excitation, or it could be intrinsically broad due to hybridization. Single-crystal measurements reveal a broad, dispersionless distribution of scattering (Lynn et al. 2000), indicating that hybridization is the cause. In addition, the distribution of magnetic scattering is temperature-independent, similar to what has been observed in non-Fermi liquid systems (Aronson et al. 1995). Lister et al. (2000) have also carried out inelastic measurements on single crystals recently and find a similar distribution of scattering, but with some structure in it. Further measurements will be needed to explore these details.

## 7. Overview and future directions

The magnetic ordering of the lanthanide ions in superconducting systems has been a topic of active interest for many years. In conventional "magnetic superconductors" such as the Chevrel phase and related materials the lanthanide moments are coupled very weakly both to the metallic electrons and to each other, resulting in very low

magnetic ordering temperatures and a delicate energetic balance with superconductivity. A similar situation occurs for the layered cuprates in that the development of long-range lanthanide magnetic order also occurs at very low temperatures. In contrast to the earlier systems, though, the superconductivity in the cuprates typically occurs at much higher temperatures, and the antiferromagnetic order that develops on the lanthanide sublattice coexists with the superconducting state. Neutron scattering has revealed the nature of the magnetic ordering of the lanthanide ions in the layered 1-2-3, 2-4-8, and 2-4-7 oxide superconductors, where the separation of the lanthanide ions is much larger along the *c*-axis than along the *a*–*b* directions. This renders these materials prototypical two-dimensional (2D) magnets, and with the spin–spin interactions being relatively weak compared to the anisotropies, this generally results in Ising-like magnetic behavior. Thus in the $ErBa_2Cu_3O_7$ material, for example, there is remarkable agreement between the observed order parameter and the exact solution for the $S = \frac{1}{2}$ 2D Ising model. Another textbook example is provided by the $DyBa_2Cu_4O_8$ system, where a geometric cancellation of the already weak interactions occurs along the *c*-axis, effectively decoupling the lanthanide *a*–*b* layers. The system thus exhibits no crossover to the 3D behavior usually found below the ordering temperature, making it the best example of a 2D magnet known to date. One of the interesting avenues of exploration will be to investigate the spin dynamics of these materials, as high-quality single crystals large enough for inelastic scattering become available.

The 2-1-4 class of materials, on the other hand, provides the first examples of superconductors where the exchange interactions unambiguously dominate the lanthanide energetics, such as $Sm_2CuO_4$ which has a dipole ordering temperature that is two orders of magnitude lower than the observed ordering temperature of 6 K. Thus the traditional picture of negligible exchange being necessary for a superconducting material to simultaneously exhibit long-range magnetic order has to be abandoned. Of course, the magnetic properties of the Cu ions are also of central interest, where the magnetic fluctuations may be directly involved in the formation of the superconducting state. The question of the origin of the superconductivity has by no means been settled yet, but even if magnetic fluctuations are not at the root of the superconductivity in these high-$T_c$ materials, it is quite clear that the Cu–O layers are intimately involved in both the magnetism and superconductivity, and the striking magnetic behavior these materials display is of fundamental interest in its own right.

From the very early days of cuprate superconductors it was known that a dramatic exception to the overall behavior of these magnetic-superconductor systems occurs for Pr, and this singular exception has been the subject of extensive research. The magnetic ordering temperatures are an order of magnitude higher for Pr than for the other lanthanide materials, and consequently the magnetic coupling must be dominated by exchange. Moreover, with the exception of $Pr_2CuO_4$ where the crystal-field ground state is an isolated singlet, superconductivity is significantly affected in the Pr materials. The origins of this effect and the nature of the Pr magnetism are still under active investigation and debate, and this will certainly be an area that will receive attention from experimentalists and theorists alike.

## Acknowledgments

We would like to thank all of our collaborators who have worked with us on various aspects of these problems. We thank Taner Yildirim for providing the calculations shown in figs. 5 and 7. We would also like to thank Taner, Frederic Bourdarot, and Dan Dender for a careful reading of the manuscript. Work at Argonne is supported by the DOE-BES, Chemical Sciences under contract W-31-109-ENG-38. Work at the University of Maryland supported in part by the NSF, DMR 97-01339.

## References

Abrikosov, A.A., and L.P. Gorkov, 1961, Sov. Phys. JETP **12**, 1243.

Akimitsu, J., H. Sawa, T. Kobayashi, H. Fujiki and Y. Yamada, 1989, J. Phys. Soc. Jpn. **58**, 2646.

Allenspach, P., S.-W. Cheong, A. Dommann, P. Fischer, Z. Fisk, A. Furrer, H.R. Ott and B. Rupp, 1989, Z. Phys. B **77**, 185.

Andreev, A.V., A.I. Buzdin and R.M. Osgood, 1990, JETP Lett. **52**, 55.

Aronson, M.C., R. Osborn, R.A. Robinson, J.W. Lynn, R. Chau, C.L. Seaman and M.B. Maple, 1995, Phys. Rev. Lett. **75**, 725.

Bacon, G.E., 1975, Neutron Diffraction, 3rd Ed. (Oxford University Press, Oxford).

Birgeneau, R.J., H.J. Guggenheim and G. Shirane, 1970, Phys. Rev. B **1**, 2211.

Boothroyd, A.T., 1998, Physica B **241**–**243**, 792.

Boothroyd, A.T., 2000, J. Alloys & Compounds **303**–**304**, 489.

Boothroyd, A.T., A. Longmore, N.H. Andersen, E. Brecht and Th. Wolf, 1997, Phys. Rev. Lett. **78**, 130.

Böttger, G., P. Fisher, A. Dönni, P. Berastegui, Y. Aoki, H. Sato and F. Fauth, 1997, Phys. Rev. B **55**, 12005.

Casalta, H., P. Schleger, E. Brecht, W. Montfrooij, N.H. Andersen, B. Lebech, W.W. Schmahl, H. Fuess, R. Liang, W.N. Hardy and T. Wolf, 1994, Phys. Rev. B **50**, 9688.

Casalta, H., P. Bourges, M. D'Astuto, D. Petitgrand and A. Ivanov, 1998, Phys. Rev. B **57**, 471.

Chattopadhyay, T., and K. Siemensmeyer, 1995, Europhys. Lett. **29**, 579.

Chattopadhyay, T., P.J. Brown, D. Bonnenberg, S. Ewert and H. Maleta, 1988a, Europhys. Lett. **6**, 363.

Chattopadhyay, T., H. Maletta, W. Wirges, K. Fisher and P.J. Brown, 1988b, Phys. Rev. B **38**, 838.

Chattopadhyay, T., P.J. Brown, B.C. Sales, L.A. Boatner, H.A. Mook and H. Maletta, 1989, Phys. Rev. B **40**, 2624.

Chattopadhyay, T., O.B. Hyun and D.K. Finnemore, 1990, Solid State Commun. **73**, 721.

Chattopadhyay, T., P.J. Brown and U. Kobler, 1991a, Physica C **177**, 294.

Chattopadhyay, T., P.J. Brown, A.A. Stepanov, P. Wyder, J. Voiron, A.I. Zvyagin, S.N. Barilo, D.I. Zhigunov and I. Zobkalo, 1991b, Phys. Rev. B **44**, 9486.

Chattopadhyay, T., P.J. Brown, B. Roessli, A.A. Stepanov, S.N. Barilo and D.I. Zhigunov, 1992, Phys. Rev. B **46**, 5731.

Chattopadhyay, T., P.J. Brown and B. Roessli, 1994a, J. Appl. Phys. **75**, 6816.

Chattopadhyay, T., J.W. Lynn, N. Rosov, T.E. Grigereit, S.N. Barilo and D.I. Zhigurov, 1994b, Phys. Rev. B **49**, 9944.

Clinton, T.W., J.W. Lynn, J.Z. Liu, Y.X. Jia and R.N. Shelton, 1991, J. Appl. Phys. **70**, 5751.

Clinton, T.W., J.W. Lynn, B.W. Lee, M. Buchgeister and M.B. Maple, 1993, J. Appl. Phys. **73**, 6320.

Clinton, T.W., J.W. Lynn, J.Z. Liu, Y.X. Jia, T.J. Goodwin, R.N. Shelton, B.W. Lee, M. Buchgeister, M.B. Maple and J.L. Peng, 1995, Phys. Rev. B **51**, 15429.

Cox, D.E., A.I. Goldman, M.A. Subramanian, J. Gopalakrishnan and A.W. Sleight, 1989, Phys. Rev. B **40**, 6998.

Elschner, B., and A. Loidl, 2000, in: Handbook on the Physics and Chemistry of Rare Earths, Vol. 30, eds K.A. Gschneidner Jr, L. Eyring and M.B. Maple (Elsevier, Amsterdam) ch. 191.

Endoh, Y., M. Matsuda, K. Yamada, K. Kakurai, Y. Hidaka, G. Shirane and R.J. Birgeneau, 1989, Phys. Rev. B **40**, 7023.

Fischer, Ø., and M.B. Maple, eds, 1983, Superconductivity in Ternary Compounds, Vols. 32 and 34 of Topics in Current Physics (Springer, New York).

Fischer, P., K. Kakurai, M. Steiner, K.N. Clausen, B. Lebech, F. Hulliger, H.R. Ott, P. Brüesch and P. Unternährer, 1988, Physica C **152**, 145.

Fischer, P., B. Schmid, P. Brüesch, F. Stucki and P. Unternährer, 1989, Z. Phys. B **74**, 183.

Goldman, A.I., B.X. Yang, J. Tranquada, J.E. Crow and C.-S. Jee, 1987, Phys. Rev. B **36**, 7234.

Goodwin, T.J., R.N. Shelton, H.B. Radousky, N. Rosov and J.W. Lynn, 1997, Phys. Rev. B **55**,3297.

Guillaume, M., P. Fischer, B. Roessli, A. Podlesnyak, J. Schefer and A. Furrer, 1993, Solid State Commun. **88**, 57.

Gukasov, A.G., S.Yu. Kokovin, V.P. Plakhty, I.A. Zobkalo, S.N. Barilo and D.I. Zhigunov, 1992, Physica B **180**, 455.

Henggeler, W., T. Chattopadhyay, B. Roessli, D.I. Zhigunov, S.N. Barilo and A. Furrer, 1996, Z. Phys. B **99**, 465.

Henggeler, W., T. Chattopadhyay, B. Roessli, P. Vorderwisch, P. Thalmeier, D.I. Zhigunov, S.N. Barilo and A. Furrer, 1997, Phys. Rev. B **55**, 1269.

Hill, J.P., A. Vigliante, D. Gibbs, J.L. Peng and R.L. Greene, 1995, Phys. Rev. B **52**, 6575.

Hill, J.P., A.T. Boothroyd, N.H. Andersen, E. Brecht and Th. Wolf, 1998, Phys. Rev. B **58**, 11211.

Hsieh, W.T., K.J. Chang, W.-H. Li, K.C. Lee, J.W. Lynn, C.C. Lai and H.C. Ku, 1994a, Phys. Rev. B **49**, 12200.

Hsieh, W.T., W.-H. Li, K.C. Lee, J.W. Lynn, J.H. Shieh and H.C. Ku, 1994b, J. Appl. Phys. **76**, 7124.

Ikeda, H., and K. Hirakawa, 1974, Solid State Commun. **14**, 529.

Katano, S., R.M. Nicklow, S. Funahashi, N. Mori, T. Kobayashi and J. Akimitsu, 1993, Physica C **215**, 92.

Li, W.-H., J.W. Lynn, H.A. Mook, B.C. Sales and Z. Fisk, 1988, Phys. Rev. B **37**, R9844.

Li, W.-H., J.W. Lynn, S. Skanthakumar, T.W. Clinton, A. Kebede, C.-S. Jee, J.E. Crow and T. Mihalisin, 1989, Phys. Rev. B **40**, R5300.

Li, W.-H., J.W. Lynn and Z. Fisk, 1990, Phys. Rev. B **41**, 4098.

Li, W.-H., K.J. Chang, W.T. Hsieh, K.C. Lee, J.W. Lynn and H.D. Yang, 1993, Phys. Rev. B **48**, 519.

Li, W.-H., C.J. Jou, S.T. Shyr, K.C. Lee, J.W. Lynn, H.L. Tsay and H.D. Yang, 1994, J. Appl. Phys. **76**, 7136.

Li, W.-H., W.Y. Chuang, S.Y. Wu, K.C. Lee, J.W. Lynn, H.L. Tsay and H.D. Yang, 1997, Phys. Rev. B **56**, 5631.

Li, W.-H., S.Y. Wu, Y.-C. Lin, K.C. Lee, J.W. Lynn, S.S. Weng, I.P. Hong, J.-Y. Lin and and H.D. Yang, 1999, Phys. Rev. B **60**, 4212.

Lin, Y.-C., W.Y. Chuang, W.-H. Li, K.C. Lee, J.W. Lynn, C.L. Yang and H.C. Ku, 1997, J. Appl. Phys. **81**, 4940.

Lin, Y.C., S.Y. Wu, W.-H. Li, K.C. Lee, J.W. Lynn, C.W. Lin, J.Y. Lin and H.D. Yang, 1998, Physica B **241**–**243**, 702.

Lister, S.J.S., A.T. Boothroyd, N.H. Andersen, A.A. Zhokhov and A.N. Christensen, 2000, Physica B **276**, 799.

Loewenhaupt, M., P. Fabi, S. Horn, P. v. Aken and A. Severing, 1995, J. Magn. Magn. Mater. **140**–**144**, 1293.

Longmore, A., A.T. Boothroyd, C. Changkang, H. Yongle, M.P. Nutley, N.H. Andersen, H. Casalta, P. Schleger and A.N. Christensen, 1996, Phys. Rev. B **53**, 9382.

Lynn, J.W., ed., 1990, High Temperature Superconductivity (Springer, New York).

Lynn, J.W., 1992, J. Alloys & Compounds **181**, 419.

Lynn, J.W., 1997, J. Alloys & Compounds **250**, 552.

Lynn, J.W., J.A. Gotaas, R.W. Erwin, R.A. Ferrell, J.K. Bhattacharjee, R.N. Shelton and P. Klavins, 1984, Phys. Rev. Letters **52**, 133.

Lynn, J.W., W.-H. Li, Q. Li, H.C. Ku, H.D. Yang and R.N. Shelton, 1987, Phys. Rev. B **36**, R2374.

Lynn, J.W., W.-H. Li, H.A. Mook, B.C. Sales and Z. Fisk, 1988, Phys. Rev. Lett. **60**, 2781.

Lynn, J.W., T.W. Clinton, W.-H. Li, R.W. Erwin, J.Z. Liu, K. Vandervoort, R.N. Shelton and P. Klavins, 1989, Phys. Rev. Lett. **63**, 2606.

Lynn, J.W., I.W. Sumarlin, S. Skanthakumar, W.-H. Li, R.N. Shelton, J.L. Peng, Z. Fisk and S.-W. Cheong, 1990, Phys. Rev. B **41**, R2569.

Lynn, J.W., S. Skanthakumar, Q. Huang, S.K. Sinha, Z. Hossain, L.C. Gupta, R. Nagarajan and C. Godart, 1997, Phys. Rev. B **55**, 6584.

Lynn, J.W., N. Rosov, S.N. Barilo, L. Kurnevitch and A. Zhokhov, 2000, Chin. J. Phys. **38**, 286.

Maletta, H., E. Pörschke, T. Chattopadhyay and P.J. Brown, 1990, Physica C **166**, 9.

Malik, S.K., S.M. Pattalwar, C.V. Tomy, R. Prasad, N.C. Soni and K. Adhikary, 1992, Phys. Rev. B **46**, 524.

Maple, M.B., 1976, Appl. Phys. **9**, 179.

Maple, M.B., 2000, in: Handbook on the Physics and Chemistry of Rare Earths, Vol. 30, eds K.A. Gschneidner Jr, L. Eyring and M.B. Maple (Elsevier, Amsterdam) ch. 187.

Matsuda, M., K. Yamada, K. Kakurai, H. Kadowaki, T.R. Thurston, Y. Endoh, Y. Hidaka, R.J. Birgeneau, M.A. Kastner, P.M. Gehring, A.H. Moudden and G. Shirane, 1990, Phys. Rev. B **42** 10098.

Matsuda, M., Y. Endoh, K. Yamada, H. Kojima, I. Tanaka, R.J. Birgeneau, M.A. Kastner and G. Shirane, 1992, Phys. Rev. B **45**, 12548.

Mook, H.A., D.McK. Paul, B.C. Sales, L.A. Boatner and L. Cussen, 1988, Phys. Rev. B **38**, 12008.

Narozhnyi, V.N., and S.-L. Drechsler, 1999, Phys. Rev. Lett. **82**, 461.

Narozhnyi, V.N., D. Eckert, K.A. Nenkov, G. Fuchs, T.G. Uvarova and K.-H. Müller, 1999, Physica C **312**, 233.

Nehrke, K., and M.W. Pieper, 1996, Phys. Rev. Lett. **76**, 1936.

Onsager, L., 1944, Phys. Rev. **65**, 117.

Paul, D.McK., H.A. Mook, A.W. Hewit, B.C. Sales, L.A. Boatner, J.R. Thompson and M. Mostoller, 1988, Phys. Rev. B **37**, 2341.

Paul, D.McK., H.A. Mook, L.A. Boatner, B.C. Sales, J.O. Ramey and L. Cussen, 1989, Phys. Rev. B **39**, 4291.

Petitgrand, D., A.H. Moudden, P. Galez and P. Boutrouille, 1990, J. Less-Common Met. **164**–**165**, 768.

Petitgrand, D., L. Boudarène, P. Bourges and P. Galez, 1992, J. Magn. Magn. Mater. **104**–**107**, 585.

Radaelli, P.G., J.D. Jorgensen, A.J. Schultz, J.L. Peng and R.L. Greene, 1994, Phys. Rev. B **49**, 15322.

Radousky, H.B., 1992, J. Mater. Res. **7**, 1917.

Roessli, B., P. Allenspach, P. Fisher, J. Mesot, U. Staub, H. Maletta, P. Brüesch, C. Ritter and A.W. Hewat, 1992, Physica B **180&181**, 396.

Roessli, B., P. Fisher, U. Staub, M. Zolliker and A. Furrer, 1993a, Europhys. Lett. **23**, 511.

Roessli, B., P. Fisher, M. Zolliker, P. Allenspach, J. Mesot, U. Staub, A. Furrer, E. Kaldis, B. Bucher, J. Karpinski, E. Jilek and H. Mutka, 1993b, Z. Phys. B **91**, 149.

Roessli, B., P. Fisher, M. Guillaume, J. Mesot, U. Staub, M. Zolliker, A. Furrer, E. Kaldis, J. Karpinski and E. Jilek, 1994, J. Phys.: Condens. Matter **6**, 4147.

Rosov, N., J.W. Lynn, G. Cao, J.W. O'Reilly, P. Pernambuco-Wise and J.E. Crow, 1992a, Physica C **204**, 171.

Rosov, N., J.W. Lynn, Q. Lin, G. Cao, J.W. O'Reilly, P. Pernambuco-Wise and J.E. Crow, 1992b, Phys. Rev. B **45**, 982.

Rosov, N., J.W. Lynn, H.B. Radousky, M. Bennahmias, T.J. Goodwin, P. Klavins and R.N. Shelton, 1993, Phys. Rev. B **47**, 15256.

Rosseinsky, M.J., K. Prassides and P. Day, 1989, J. Chem. Soc., Chem. Commun. **22**, 1734.

Rosseinsky, M.J., K. Prassides and P. Day, 1991, Inorg. Chem. **30**, 2680.

Sachidanandam, R., T. Yildirim, A.B. Harris, A. Aharony and O. Entin-Wohlman, 1997, Phys. Rev. B **56**, 260.

Skanthakumar, S., 1993, Ph.D. Thesis (University of Maryland).

Skanthakumar, S., and L. Soderholm, 1996, Phys. Rev. B **53**, 920.

Skanthakumar, S., H. Zhang, T.W. Clinton, W.-H. Li, J.W. Lynn, Z. Fisk and S.-W. Cheong, 1989, Physica C **160**, 124.

Skanthakumar, S., W.-H. Li, J.W. Lynn, A. Kebede, J.E. Crow and T. Mihalisin, 1990, Physica B **163**, 239.

Skanthakumar, S., J.W. Lynn, J.L. Peng and Z.Y. Li, 1991, J. Appl. Phys. **69**, 4866.

Skanthakumar, S., J.W. Lynn, J.L. Peng and Z.Y. Li, 1992, J. Magn. Magn. Mater. **104**–**107**, 519.

Skanthakumar, S., J.W. Lynn, J.L. Peng and Z.Y. Li, 1993a, J. Appl. Phys. **73**, 6326.

Skanthakumar, S., J.W. Lynn, J.L. Peng and Z.Y. Li, 1993b, Phys. Rev. B **47**, R6173.

Skanthakumar, S., J.W. Lynn and F. Dogan, 1997a, J. Appl. Phys. **81**, 4934.

Skanthakumar, S., J.W. Lynn, N. Rosov, G. Cao and J.E. Crow, 1997b, Phys. Rev. B **55**, R3406.

Skanthakumar, S., J.W. Lynn, J.L. Peng and Z.Y. Li, 1999, private communication.

Soderholm, L., S. Skanthakumar and C.W. Williams, 1999, Phys. Rev. B **60**, 4302.

Stassis, C., and A.I. Goldman, 1997, J. Alloys & Compounds **250**, 603.

Staub, U., and L. Soderholm, 2000, in: Handbook on the Physics and Chemistry of Rare Earths, Vol. 30, eds K.A. Gschneidner Jr, L. Eyring and M.B. Maple (Elsevier, Amsterdam) ch. 194.

Staub, U., L. Soderholm, S. Skanthakumar and M.A. Antonio, 1995, Phys. Rev. B **52**, 9736.

Staub, U., L. Soderholm, S. Skanthakumar, S. Roskenkranz, C. Ritter and W. Kagunya, 1996, Europhys. Lett. **34**, 447.

Staub, U., L. Soderholm, S. Skanthakumar, S. Roskenkranz, C. Ritter and W. Kagunya, 1997, Z. Phys. B **104**, 37.

Sumarlin, I.W., S. Skanthakumar, J.W. Lynn, J.L. Peng, W. Jiang, Z.Y. Li and R.L. Greene, 1992, Phys. Rev. Lett. **68**, 2228.

Sumarlin, I.W., J.W. Lynn, T. Chattopadhyay, S.N. Barilo and D.I. Zhigunov, 1994, Physica C **219**, 195.

Sumarlin, I.W., J.W. Lynn, T. Chattopadhyay, S.N. Barilo, D.I. Zhigunov and J.L. Peng, 1995, Phys. Rev. B **51**, 5824.

Thalmeier, P., 1996, Physica C **266**, 89.

Thomlinson, W., G. Shirane, J.W. Lynn and D.E. Moncton, 1983, in: Superconductivity in Ternary Compounds, eds M.B. Maple and Ø. Fischer, Vol. 34 of Topics in Current Physics (Springer, New York) ch. 8.

Thurston, T.R., M. Matsuda, K. Kakurai, K. Yamada, Y. Endoh, R.J. Birgeneau, P.M. Gehring, Y. Hidaka, M.A. Kastner, T. Murakami and G. Shirane, 1990, Phys. Rev. Lett **65**, 263.

Uma, S., W. Schnelle, E. Gmelin, G. Rangarajan, S. Skanthakumar, J.W. Lynn, R. Walter, T. Lorenz, B. Bucher and A. Erb, 1998a, J. Phys. (Lett.) **10**, L33.

Uma, S., G. Rangarajan and E. Gmelin, 1998b, Physica C **301**, 141.

Vaknin, D., S.K. Sinha, D.E. Moncton, D.C. Johnston, J.M. Newsam, C.R. Safinya and H.E. King Jr, 1987, Phys. Rev. Lett. **58**, 2802.

Vaknin, D., S.K. Sinha, C. Stassis, L.L. Miller and D.C. Johnston, 1990, Phys. Rev. **41**, 1926.

Vaknin, D., L.L. Miller and J.L. Zarestky, 1997, Phys. Rev. B **56**, 8351.

Vigoureux, P., M. Braden, A. Gukasov, W. Paulus, P. Bourges, A. Cousson, D. Petitgrand, J.P. Lauriat, M. Meven, S.N. Barlio, D. Zhigunov, P. Adelmann and G. Heger, 1997a, Physica C **273**, 239.

Vigoureux, P., A. Gukasov, S.N. Barlio and D. Zhigunov, 1997b, Physica B **234**–**236**, 815.

Wang, H.Y., C.H.Chang, S.R. Hwang, W.-H. Li, K.C. Lee, J.W. Lynn, H.M. Luo and H.C. Ku, 2000, Phys. Rev. B **62**, 11549.

Wu, S.Y., W.T. Hsieh, W.-H. Li, K.C. Lee, J.W. Lynn and H.D. Yang, 1994, J. Appl. Phys. **75**, 6598.

Wu, S.Y., W.-H. Li, K.C. Lee, J.W. Lynn, T.H. Meen and H.D. Yang, 1996, Phys. Rev. B **54**, 10019.

Xiong, Y.F., Y.S. Yao, L.F. Xu, F. Wu, D. Jin and Z.X. Zhao, 1998, Solid State Commun. **107**, 509.

Yamada, K., M. Matsuda, Y. Endoh, B. Keimer, R.J. Birgeneau, S. Onodera, J. Mizusaki, T. Matsuura and G. Shirane, 1989, Phys. Rev. B **39**, 2336.

Yang, K.N., J.M. Ferreira, B.W. Lee, M.B. Maple, W.-H. Li, J.W. Lynn and R.W. Erwin, 1989, Phys. Rev. B **40**, 10963.

Yildirim, T., 1999, Turk. J. Phys. **23**, 47.

Yildirim, T., A.B. Harris, O.E. Wohlman and A. Aharony, 1994, Phys. Rev. Lett. **72**, 3710.

Yildirim, T., A.B. Harris and E.F. Shender, 1996, Phys. Rev. B **53**, 6455.

Yildirim, T., S. Skanthakumar and J.W. Lynn, 1998, private communication.

Zhang, H., J.W. Lynn, W.-H. Li, T.W. Clinton and D.E. Morris, 1990, Phys. Rev. B **41**, 11229.

Zhang, H., J.W. Lynn and D.E. Morris, 1992, Phys. Rev. B **45**, 10022.

Zobkalo, I.A., A.G. Gukasov, S.Yu. Kokovin, S.N. Barilo and D.I. Zhigunov, 1991, Solid State Commun. **80**, 921.

Zou, Z., J. Ye, K. Oka and Y. Nishihara, 1998, Phys. Rev. Lett. **80**, 1074.

Zou, Z., J. Ye, K. Oka and Y. Nishihara, 1999, Phys. Rev. Lett. **82**, 462.